Construction and characterization of inert misfolded protein models in transformed mammalian cells

Ph.D. Thesis

Mehmet Alper Arslan M.Sc.

Semmelweis University
Molecular Medicine Doctoral School

Supervisor: Dr. Sőti Csaba M.D., Ph.D.

Reviewers: Dr. Chinopoulos Christos M.D., Ph.D.
Dr. Mihalik Rudolf M.D., Ph.D.

Exam board chair: Dr. Kolev Kraszimir M.D., Ph.D., D.Sc.
Exam board members: Dr. Kardos József Ph.D.
Dr. Gábor Petheő M.D., Ph.D.

Budapest
2012

Table of Contents

Abbreviations

Aβ	Amyloid-β
ALS	Amyotrophic lateral sclerosis
APP	Amyloid precursor protein
ATP	Adenosine triphosphate
BAG	Bcl-2 associated athanogene
BCA	Bicinchoninic acid
BrdU	5-bromo-2'-deoxyuridine
BSA	Bovine serum albumin
CAT	Chloramphenicol acetyltransferase
CBP	CREB (cyclic AMP response element-binding protein)-binding protein
cBSA	cytosolic bovine serum albumin
CFTR	Cystic fibrosis transmembrane conductance regulator
CHIP	Carboxyl-terminus of Hsc70-interacting protein
CMA	Chaperone-mediated autophagy
CMV	Cytomegalovirus
COS-7	CV-1 with an origin-defective mutant of SV40
Cy3	Cyanine 3
DAPI	4',6-diamidino-2-phenylindole
ddSIRT1	deacetylase-deficient mutant (H363Y) form of SIRT1
DMEM	Dulbecco’s modified Eagle’s medium
DMSO	Dimethyl sulfoxide
DNA	Deoxyribonucleic acid
DTNB	5,5'-dithiobis-(2-nitrobenzoic acid)
ECL	Enhanced chemiluminescence
EGFP	Enhanced green fluorescent protein
ER	Endoplasmic reticulum
FBS	Fetal bovine serum
FITC	Fluorescein isothiocyanate
GFP	Green fluorescent protein

GFP170*	GFP fused to an internal fragment of the Golgi complex protein 170
HCl	Hydrochloric acid
HEK-293	Human embryonic kidney cells 293
HEPES	4-(2-hydroxyethyl)-1-piperazineethanesulfonic acid
HRP	Horseradish peroxidase
HSE	Heat shock element
HSF1	Heat shock factor 1
Hsp	Heat shock protein
HSR	Heat shock response
JNK	c-Jun N-terminal kinase
luc	Firefly luciferase/luminescence
MG-132	carbobenzoxy-L-leucyl-L-leucyl-L-leucinal
NAD^+	Nicotinamide-adenine dinucleotide
NMR	Nuclear magnetic resonance
PAGE	Polyacrylamide gel electrophoresis
PBS	Phosphate-buffered saline
PCR	Polymerase chain reaction
PI	Propidium iodide
polyQ	polyglutamine
rGFP	recombinant GFP
RNase A	Ribonuclease A
ROS	Reactive oxygen species
SCA	Spinocerebellar ataxia
SDS	Sodium dodecyl sulfate
siRNA	small/short interfering ribonucleic acid
SIRT1	Silent information regulator 2 (Sir2)-type protein 1
SNP	Single nucleotide polymorphism
SOD1	Superoxide dismutase 1
SV40	Simian virus 40
TBP	TATA-box binding protein
TBS	Tris-buffered saline

TK	Thymidine kinase
Tris	Tris(hydroxymethyl)aminomethane
UPR	Unfolded protein response
UPS	Ubiquitin-proteasome system
UV	Ultraviolet
YFP	Yellow fluorescent protein
wt	wild-type
β-gal	β-galactosidase
Δ9CAT	C-terminal 9 amino acid-truncated form of CAT
3-MA	3-methyladenine

1. Introduction

1.1. Protein misfolding and aggregation in postmitotic cells

Protein misfolding is a distinctive characteristic feature of a large group of diseases known as protein conformational diseases as well as aging [1-2]. Proteins may misfold due to inherent mutations [1], mistranslation [3], post-translational modifications (i.e. oxidation, nitration, phosphorylation, glycation, proteolytic cleavage) [4-6], and upon denaturing stress (i.e. heat, heavy metals, acidic pH) [7]. Protein misfolding results in loss of native structure and exposure of hydrophobic stretches that are normally buried within the native globular fold. These sticky misfolded species tend to associate with each other via hydrogen bonding and result in soluble oligomers with a cross β-sheet structure [8]. The process of nucleation-dependent polymerization and aggregation goes on until large inclusion bodies and the so-called aggresomes [9] are formed at distinct cellular locations. Therefore, protein aggregation can be considered as a complex multi-step process starting from single monomers and ending in large bodies of insoluble protein aggregates [8].

Protein misfolding is implicated in the postmitotic compartment and in aging. Conformational diseases arise from misfolding and aggregation of specific proteins in postmitotic tissues including the liver, skeletal muscle, eye lens and the brain [10]. Our knowledge on protein aggregation comes largely from studies on neurodegenerative disease models. Although specific abnormal proteins responsible for the pathogenesis are completely different in sequence, structure and function, all neurodegenerative disorders share the common end-stage of protein aggregation and deposition, which take place at various cellular locations (cytoplasm, nucleus or extracellular space) within discrete neuronal regions of the brain [1]. Huntington's disease is caused by an expanded CAG repeat in huntingtin gene and manifests when the length of glutamine in the encoded protein exceeds a threshold level of 36-40 [6]. Intranuclear and to a lesser extent cytoplasmic inclusions of the aggregated huntingtin protein in the striatum are a

pathological hallmark of the disease. Spinocerebellar ataxia (SCA) is another neurodegenerative polyglutamine (polyQ) disease affecting mainly the cerebellum, which is caused by an expanded glutamine repeat in *SCA* gene product, ataxin. Alzheimer's disease is characterized by two types of lesions in the hippocampus and neocortex: extracellular plaques made up of aggregates of amyloid-β (Aβ) peptide that is derived from two proteolytic cleavages of the transmembrane amyloid precursor protein (APP), and intracellular tangles composed of aggregates of hyperphosphorylated microtubule-associated protein tau [11]. The characteristic lesion of Parkinson's disease, the so-called Lewy body, is a juxtanuclear cytoplasmic inclusion body comprised largely of aggregated α-synuclein protein and ubiquitin-protein ligase parkin [12]. Lewy bodies are densest in the substantia nigra of the midbrain where they are particularly associated with the degeneration of dopaminergic neurons. Familial amyotrophic lateral sclerosis (ALS) is caused by mutations in the antioxidant enzyme superoxide dismutase (SOD1), which tend to aggregate as cytoplasmic inclusions in motor neurons of the brainstem, spinal cord and cerebral cortex [6].

Although the term 'amyloid' was originally coined to describe the extracellular deposits found in Alzheimer's disease, it has now become a generic term that refers to detergent-insoluble protein aggregates, organized in highly ordered cross-β structure and show fibrillar appearance under electron microscopy [1]. Amyloid fibrils typical of many neurodegenerative diseases are filamentous, unbranched straight structures with a diameter of ~10 nm and a length of 0.1-10 μm [8]. X-ray fiber diffraction pattern analysis and solid-state NMR studies have revealed that the core structure of the amyloid fibril is composed of β-sheets whose strands run perpendicular to the fibril axis with hydrogen bonds running almost parallel to the long axis [13-14]. Aggregation with an ultrastructure of amyloid fibrils is a common feature of the otherwise unrelated neurodegenerative disease-associated proteins such as amyloid-β [15], α-synuclein [16], huntingtin [17] and SOD1 [18] with an exception of tau aggregates, which is mainly composed of α-helices [19]. Interestingly, the ability of polypeptide chains to form amyloid structures seems not to be restricted to these particular disease-related abnormal proteins. Under appropriate solution conditions (e.g. at low pH) where the native fold of a protein is partially

destabilized with hydrogen bonding remaining still favorable [20], fibrils indistinguishable from those found in amyloid diseases can be formed *in vitro* by many other proteins, including well-known molecules such as myoglobin and insulin, and also by polypeptides like polythreonine or polylysine [8, 21]. This seemingly generic feature of polypeptide chains can be justified by the fact that hydrogen bonds stabilizing the β-sheet structure of amyloid fibrils also involve the main chain (polypeptide backbone), which is common to all polypeptides [8]. This observation also helps explain why amyloid fibrils formed from diverse, structurally unrelated disease-associated proteins all look morphologically similar regardless of sequence. Indeed, herein lies the still unresolved mystery of *in vivo* protein aggregation: if the ability to form amyloid fibrils is generic, then why are the aforementioned particular proteins more prone to misfold and aggregate in distinct neurodegenerative disorders? Answers to this question may lie in different intrinsic physicochemical properties of these proteins (e.g. charge, hydrophobicity, secondary-structure propensities within themselves or after a post-translational modification) [8, 22], and/or cell type-specific and even cell-to-cell variations in external factors, particularly the capacity of defense mechanisms (i.e. refolding and degradation/clearance) [1], which will be discussed in Section 1.4.

Formation of amyloid fibrils represents only a late-intermediate stage in the cascade of events leading to protein aggregation. The process of fibrillogenesis *in vivo* seems to be a complex phenomenon that is structurally hard to study due to the unstable and transient nature of intermediate species generated. Therefore, much of the knowledge that is currently available comes from *in vitro* biophysical studies mostly performed with amyloid-β [23-24] and polyglutamine [25-26]. Destabilization of the normal protein conformation due to intrinsic and/or environmental factors starts the process by exposing hidden hydrophobic segments, which then seems to follow a self-driven pathway of nucleation/seeding-dependent polymerization (Fig. 1). Initially abnormal, unstable monomeric proteins associate with each other and stabilize in a β-sheet structure to form soluble, bead-like globular oligomers often described as amorphous aggregates. These early pre/non-fibrillar oligomers then link together and grow into fibrillar, yet still soluble species termed protofibrils [27]. Protofibrils are unbranched, rod-like structures that are

3-6 nm wide and up to 100 nm long as studied by electron microscopy and atomic force microscopy [28-29]. Possibly through lateral interactions, protofibrils intertwine and transform into long, highly insoluble amyloid fibrils [28-29], which eventually accumulate in large inclusion bodies or aggresomes even visible under light microscope [30]. This general model for fibrillogenesis based on sequential, hierarchical order of assembly [31] may not mimic the *in vivo* situation in human diseases, which is likely to be more complicated and still remains to be resolved by future studies.

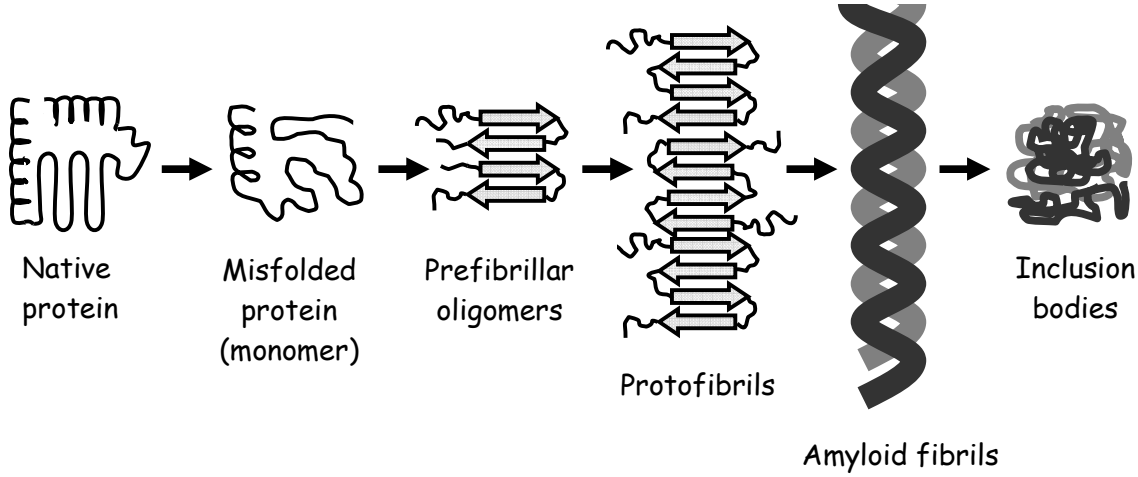

Figure 1. The process of amyloid fibril formation (fibrillogenesis). Proteins may misfold due to environmental stress, mutations, posttranslational modifications or translational errors. The pathway of protein aggregation starts when a native protein undergoes a structural transition into a misfolded abnormal conformation. Monomeric misfolded proteins expose previously hidden hydrophobic segments, which tend to associate with each other and stabilize in a β-sheet structure to form prefibrillar oligomers. Once formed, these oligomeric species rapidly polymerize to give rise to protofibrils. Amyloid fibrils can then form via self-assembly of protofibrillar intermediates, which finally results in formation of large aggregates known as inclusion bodies even visible under light microscope. Molecular components are not drawn to scale (modified from refs. [1, 6, 8]). Note that soluble monomers and oligomeric or protofibrillar intermediates are thought to be the species causing cytotoxicity, whereas the insoluble amyloid fibrils and inclusion bodies as the end products of aggregation are considered to serve a cytoprotective role (see Section 1.2).

1.2. Nature of the toxic species in neurodegeneration

Neurodegeneration is typically characterized by selective neuronal cell death by apoptosis, impaired synaptic plasticity and neuroinflammation [32]. As being the most visibly common feature of all neurodegenerative diseases, amyloid fibrils and inclusion bodies were initially assumed to be the toxic species causing neurodegeneration. However, lack of correlation between the presence of inclusion bodies and the markers of neuropathology has not supported this hypothesis. For example, in Huntington's disease, although inclusion bodies are denser in the cerebral cortex than in the cells of striatum, only a moderate degeneration is detected in the cortex [33], and polyglutamine aggregates may not be a predictor of cell loss in the striatal neurons [34]. More direct evidence regarding the role of huntingtin aggregates in neuronal cell death has come from cell culture models where the exposure of mutant huntingtin-transfected striatal neurons to conditions that suppress the formation of inclusions resulted even in an increase in mutant huntingtin-induced death [35]. These findings suggest that inclusion bodies may even be protective and early stages of oligomerization might be the real culprits of cytotoxicity in neurodegeneration (Fig. 1). Similar findings have been reported in different studies conducted with other neurodegenerative diseases. There seems to be a poor correlation between Alzheimer's disease dementia and amyloid plaques [36]. Morphological and biochemical analyses of the brains of people affected by Parkinson's disease have shown that the presence of Lewy bodies does not predispose a neuron to undergo apoptosis [37]. SCA1 transgenic mice deficient in forming nuclear ataxin-1 aggregates due to deletion within the self-assembly region developed ataxia and Purkinje cell pathology similar to the original SCA1 mice, indicating that ataxin-1 aggregation is not required to initiate pathogenesis [38].

In search of the primary toxic species of neurodegeneration, two initial reports on amyloid-β protein rightly drew the attention away from mature amyloid fibrils and inclusions to two soluble intermediates of fibrillogenesis, namely nonfibrillar oligomers [39] and protofibrils [40] (Fig. 1). Later, these amyloid-β-derived oligomers have been specifically shown to induce cytotoxicity in rats *in vivo* through inhibition of

hippocampal long-term potentiation, a paradigm of synaptic plasticity [41]. Natural accumulation of such soluble oligomers in Alzheimer's disease-affected brain has subsequently been verified using antibodies raised against synthetic amyloid-β oligomers [42], and these neutralizing antibodies seem to offer promising therapeutic benefits [43]. Strong association of soluble nonfibrillar oligomers with neuropathogenesis has been demonstrated by further studies performed with other neurodegenerative disease models. For example, specific inhibition of polyglutamine oligomerization as well as disruption of preformed oligomers by infusion of the amyloid-binding azo-dye Congo red into a transgenic mouse model of Huntington's disease exerts marked protective effects on survival and motor function [44]. In *Sca1* gene-targeted mice harboring extra glutamine repeats in the endogenous ataxin-1, most adversely affected neurons were the ones containing the most soluble mutant ataxin-1, indicating that neurons that cannot sequester the mutant protein in large aggregates suffer the worst damage from polyglutamine-induced toxicity [45]. Indeed, inclusion body formation has directly been associated with reduced risk of neuronal death in cell culture models of Huntington's [46] and Parkinson's diseases [47], suggesting the formation of inclusion bodies might represent a cytoprotective mechanism to sequester and segregate toxic misfolded intermediates out of harm's way.

1.3. Mechanisms of cytotoxicity in neurodegeneration

Microscopic analysis of the globular nonfibrillar aggregates derived from diverse disease-related proteins (i.e. huntingtin, CFTR of cystic fibrosis, amyloid-β, α-synuclein) by purification from either mammalian cells [48] or *E. coli* [49] has revealed morphologically similar ultrastructures for these species. The concept of a common structure has further been supported by evidence that a single monoclonal antibody raised against a soluble amyloid-β oligomer also cross-reacts with nonfibrillar oligomeric, but *not* with monomeric or mature fibrillar forms of polyglutamine, α-synuclein and prion proteins, and cytotoxicity of these prefibrillar aggregates can be efficiently suppressed by the same antibody [50]. Interestingly, *in vitro*-generated granular nonfibrillar, but *not*

mature fibrillar aggregates of even non-disease-associated proteins, namely SH3 domain from bovine phosphatidyl-inositol-3'-kinase and the amino terminal domain of the *E. coli* HypF protein, have been found to be highly cytotoxic when added to the cell culture medium [51]. Taken together, these studies indicate that like mature amyloid fibrils, prefibrillar globular aggregates also share a common structure irrespective of the sequence, structure or function of the original protein. However, unlike the mature fibrils, prefibrillar aggregates possess an inherently toxic character, which is attributable to their common structural nature rather than to the specific sequences of the original proteins, implying a common mechanism of cytotoxicity for diverse protein misfolding diseases [51]. Indeed, such a toxic gain-of-function seems more likely to develop in these prefibrillar aggregates, as misfolding-induced exposure of hydrophobic side-chains will be much more accessible on their surface than in the fully formed mature fibrils [51].

Exposure of non-native hydrophobic surfaces has been proposed to account for the molecular basis of aggregate toxicity by permitting incorrect protein-protein interactions with other essential cellular components [51], leading successively to their inhibition, loss of function, sequestration into larger aggregates and depletion. Indeed, certain transcription factors [52-53], cell cycle regulators like p53 [54-55], molecular chaperones Hsp70 and Hsp40 [54, 56-57], cytoskeletal proteins [54], ubiquitin [58-59] and subunits of the proteasome [56-57] have been found to be present in fibrillar aggregates from diverse neuropathologies. Among these, the pro-survival transcription factors CBP (CREB-binding protein) [52] and TBP (TATA-box binding protein) [53] are of particular interest, as they themselves contain a short, benign polyglutamine (polyQ) stretch, which interacts specifically with the expanded polyQ tract of soluble, oligomeric mutant huntingtin, possibly in a polar zipper motif. This interaction, independently of the formation of insoluble coaggregates, structurally destabilizes the transcription factors, causing transcriptional abnormalities that eventually culminate in cellular toxicity [52-53] (Fig. 2). However, transcription factor inactivation does not seem necessarily to originate from a polyQ–polyQ interaction, as the tumor-suppressor protein p53, devoid of any polyQ tract *per se*, has also been reported to interact with the pathogenic polyQ region of mutant huntingtin, resulting in transcriptional repression of the p53-regulated protein

p21$^{WAF1/CIP1}$ [55]. Interestingly, nuclear aggregates of even a non-polyQ protein GFP170*, a fusion of GFP to an internal fragment of the Golgi complex protein 170 (GCP170), can recruit transcription factors such as CBP and p53, and repress p53 transcriptional activity, implying transcriptional dysregulations may represent a common deleterious consequence of nuclear protein aggregation, irrespective of the polyQ content of the original protein [60] (Fig. 2).

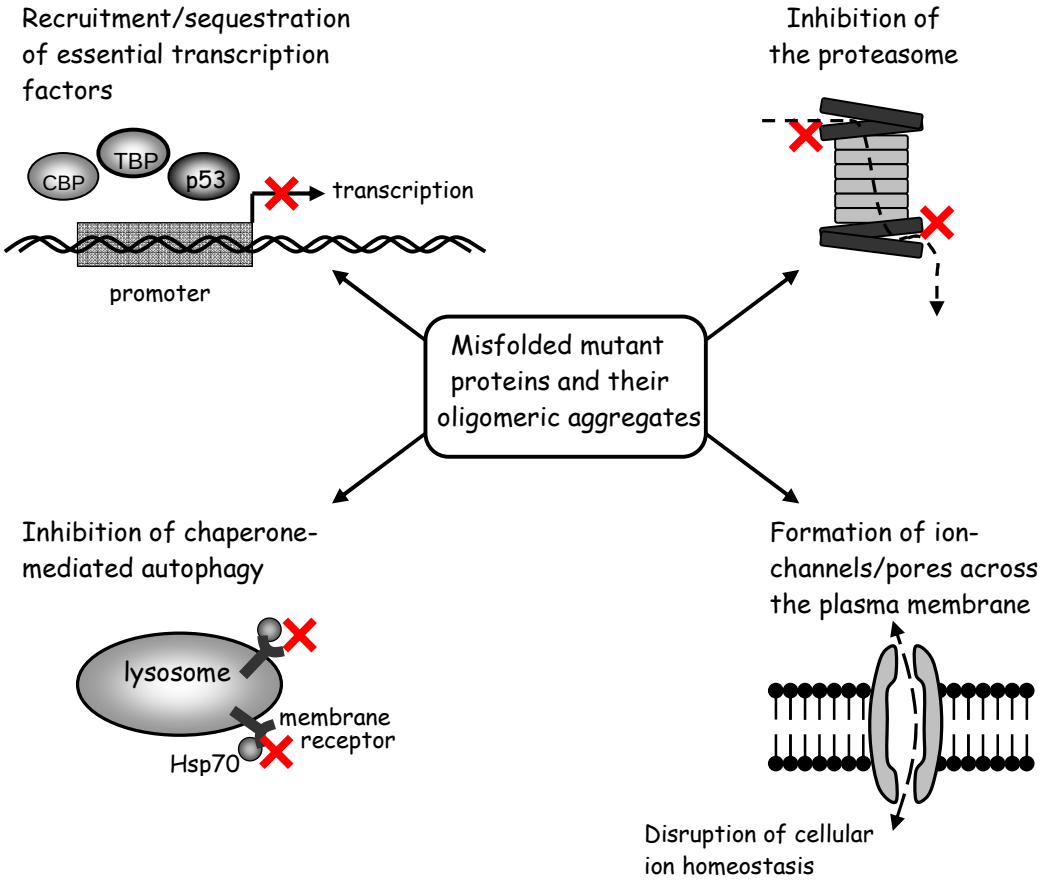

Figure 2. Cytotoxic mechanisms of misfolded proteins and their oligomeric (intermediate) aggregates. The molecular basis of aggregate toxicity is the incorrect interactions of monomeric/oligomeric species of misfolded proteins with essential cellular components such as transcription factors, proteasomes, lysosomes and the plasma membrane. Such aberrant interactions lead to sequestration and/or inhibition of these key elements (indicated by crosses), compromising a diverse set of cellular functions. Aggregation intermediates may also interact with the plasma membrane and form ion-channel-like pores, disrupting the integrity of cell membrane, which results in altered ion homeostasis and eventually lead to cell death. (modified from ref. [1])

Another mechanism by which protein aggregation is linked to cytotoxicity is through strong inhibition of the ubiquitin-proteasome system (UPS) [61], a key regulator of almost all aspects of cellular function such as gene expression, cell division, signal transduction and apoptosis [62] (Fig. 2). Transient overexpression of two unrelated aggregation-prone proteins (i.e. mutant CFTR and expanded polyQ fragment of huntingtin) in HEK-293 cells stably expressing a novel GFP-based reporter of UPS activity, a C-terminal fusion of GFP to a 16-residue degron peptide, has revealed that the function of the UPS is severely impaired in cells with large inclusion bodies [61]. This unstable GFP variant that normally undergoes proteasome-dependent degradation was reported to accumulate specifically in cells with aggresomes, as evidenced by substantial increases in intracellular GFP fluorescence levels [61]. Moreover, protein aggregation has also caused a cell cycle arrest at the G2/M boundary in these cells [61]. Moreover, a subsequent study by the same group has extended the above finding by showing that UPS inhibition associated with protein aggregation is global and can also be observed in the absence of any detectable inclusion bodies, suggesting that intermediate forms of protein aggregates not visible by microscopy, such as small oligomers or protofibrils, might be the toxic species responsible for UPS impairment [63]. It is likely that once an aggregation-prone soluble monomeric protein has escaped degradation by the UPS, the oligomeric species generated may prove hard to be unfolded by the 19S regulatory complex and fail to fully enter the 20S catalytic core, causing the associated proteasomes to become trapped in the growing aggregates [64]. Indeed, certain aggregation-prone proteins (i.e. polyglutamine proteins) have been shown to be intrinsically resistant to degradation by the eukaryotic proteasome both *in vitro* and *in vivo* [65-66], with the shorter polyQ sequences released undigested. This finding has prompted the proposal that occasional failure of longer (disease-related), undegradable polyQ sequences to exit might result in kinetically trapped reactive substrates within the proteasomes. In both mutually non-exclusive cases presented above (i.e. hard-to-unfold oligomers or degradation-resistant monomers), the common outcome would be direct inhibition and choking of the 26S proteasomes (Fig. 2), followed in time by their irreversible sequestration into large aggregates [66-67] and depletion from their cellular sites of action. Alternatively, the formation of highly ubiquitylated protein aggregates, a typical

characteristic of inclusion bodies, has been proposed to cause a relative shortage of free ubiquitin levels, and thereby indirectly impair the UPS function, which requires a prior polyubiquitin tagging for any aberrant protein to be degraded [62]. Indeed, during proteotoxic stress (i.e. proteasome inhibition), ubiquitin has been shown to be redistributed due to substrate competition for a limited pool of free ubiquitin, as evidenced by accumulation of polyubiquitylated abnormal proteins coinciding with depletion of monoubiquitylated histone H2A and chromatin remodeling [68]. Although not supported by other studies [61, 63], if correct, such a rate-limiting pool might also lead to dysfunction in other ubiquitin-dependent cellular processes that range from transcriptional regulation to membrane protein transport [69]. In fact, since ubiquitylation of misfolded proteins directly precedes their degradation by the UPS [62], the observation that inclusion bodies are invariably enriched with ubiquitin and proteasome subunits [56-59] has long suggested a potential role for dysfunctional UPS in neurodegeneration. Therefore, whatever the underlying mechanisms are, UPS impairment seems to start a vicious cycle where inhibitors of the system are at the same time the products that result from its own inhibition, which might help explain the often precipitous nature of neurodegenerative disease progression [61].

Besides the UPS, another degradative machinery of cells, chaperone-mediated autophagy (CMA), has also been reported to be inhibited by aggregation-prone mutant proteins [70]. Two mutant pathogenic forms of α-synuclein were shown to bind to and block the lysosomal membrane receptor of CMA, inhibiting both their own degradation and that of other CMA substrates [70], which is likely to have some more toxic consequences for the cell, in addition to those arising from promotion of their own aggregation (Fig. 2). Although blockade of CMA leads to a compensatory upregulation of another major form of autophagy, macroautophagy, it seems to fail to compensate for all CMA functions, as demonstrated by CMA-deficient cells displaying an increased susceptibility to various damaging stressors such as UV and oxidative stress [71].

Formation of ion channel-like structures across the plasma membrane by globular nonfibrillar and protofibrillar aggregates from different amyloid proteins including

amyloid-β and α-synuclein has been proposed as yet another mechanism for cellular toxicity associated with protein aggregation [72-73]. Disruption of the integrity of cell membrane by such spontaneously formed pores was shown to cause an imbalance of ion homeostasis (Fig. 2), particularly a sharp increase in intracellular Ca^{2+} levels [74-75], which may eventually lead to cell death via interference with various signal transduction pathways [76]. Interestingly, similar results were obtained with cells exposed to *in vitro*-generated prefibrillar aggregates of even a non-disease-associated bacterial protein HypF in their culture medium [77]. Although the mechanism of aggregate translocation into the cells has not been fully investigated in this study [77], taken together, inappropriate membrane permeabilization seems to represent another common cytotoxic mechanism inherent to the structural nature of protein aggregation, irrespective of the origin of the aggregated protein [51, 77].

1.4. Proteostasis and defense mechanisms against protein aggregation

As all proteins seem to possess an inherent tendency to misfold and aggregate, protein aggregation is a continuous threat to cells even in the absence of any pathological condition [8, 78]. Indeed, exposure of non-native hydrophobic regions by nascent polypeptides during *de novo* protein synthesis and later by partially folded intermediates is a frequent event in the lifetime of many proteins until they attain their native, three-dimensional structure [79]. Even native proteins are at permanent risk of misfolding, unfolding and denaturation, particularly under environmental stress conditions, such as heat and oxidative stress [7, 80]. If left unattended, such hydrophobic surfaces can seed aggregation [81], and lead to inappropriate homotypic or heterotypic protein-protein interactions within the highly crowded macromolecular environment of the cell [82], which would eventually produce a toxic and even deadly consequence for the cell, as has been discussed above in Section 1.3. Cells of all living systems have therefore evolved natural defense mechanisms against protein misfolding and aggregation, which act either to facilitate folding or refolding of misfolded proteins by molecular chaperones or to remove them by proteolytic degradation pathways including the ubiquitin-proteasome

system (UPS) and lysosome-mediated autophagy [80]. A proper balance between these protein quality control systems constitutes the central element of protein homeostasis, also referred to as proteostasis [83]. Protein aggregation seems to result from failure and/or exhaustion of the above quality control systems due to genetic mutations in the components of these systems or chronic proteotoxic stress, as both concomitantly occur during aging [7, 80].

1.4.1. Molecular chaperones and the heat shock response

Molecular chaperones, many of which are designated as heat shock proteins (Hsp-s), provide the main line of defense against protein misfolding in cells. Many chaperones can passively bind and shield non-native hydrophobic surfaces exposed by misfolded and partially unfolded proteins, preventing aberrant inter- and intramolecular interactions as well as aggregation [7]. Certain chaperones like Hsp70 can actively refold misfolded proteins through cycles of binding and release in an ATP-dependent manner [79]. Hsp70 works in tight coordination with other chaperones and co-chaperones, which play key roles in determining the fate of the bound misfolded proteins. For example, the co-chaperone Hsp40 stimulates the ATPase activity of Hsp70, thereby keeping the bound substrates in successive refolding cycles [79, 84] (Fig. 3). Hsp40 also functions to deliver a diverse set of substrates to Hsp70 and determines substrate specificity, including sequences not containing hydrophobic amino acids, which may help explain recognition of expanded polyQ regions by Hsp70 [64, 85]. Prolonged association of misfolded proteins with the Hsp70-Hsp40 system is interpreted as a failure of refolding/repair [84, 86], and leads to recruitment of another co-chaperone, CHIP (carboxyl-terminus of Hsc70 interacting protein), which functions both as a negative regulator of chaperone activity [87] and an E3 ubiquitin ligase [88]. Inhibition of the ATPase activity of Hsp70 interrupts unsuccessful refolding cycles and enables CHIP to ubiquitylate the terminally misfolded, irreparably/irreversibly damaged proteins, thereby targeting them for degradation by the 26S proteasome [89]. Binding to the 26S proteasome is mediated by an additional co-chaperone, BAG1 (Bcl-2 associated athanogene 1), which also interacts

both with CHIP and Hsp70 [90-91]. Therefore, co-chaperones CHIP and BAG1 provide a physical link between Hsp70 and the proteasome, and cooperate to switch the activity of the Hsp70 system from protein (re)folding to protein degradation by the UPS (Fig. 3). More interestingly, it has recently been shown that when the UPS is impaired, CHIP-bound Hsp70 changes its co-chaperone partner from BAG1 to BAG3, and thereby directs misfolded substrate proteins in a microtubule-dependent manner to aggresomes [92-93], which can later be cleared by macroautophagy [80]. As the inclusion bodies are considered to serve a cytoprotective role by sequestering toxic soluble oligomers (discussed above in Section 1.2), promoting their formation under stress conditions (i.e. UPS inhibition) seems to be in good consistency with a generic cytoprotective function of Hsp70. Although yet poorly understood, association of the Hsp70 system with macroautophagy is likely to provide this clearance mechanism with a chaperone-mediated specificity towards misfolded proteins, and implies even a broader role for Hsp70 in autophagy than that observed by sequence-specific targeting of only certain cytosolic proteins to lysosomes, a specialized degradative pathway known as chaperone-mediated autophagy (CMA) [94]. Furthermore, apart from its pro-aggregation function, Hsp70 can also act together with the Hsp100 class of chaperones to disaggregate and resolubilize pre-existing aggregates in yeast [95] and bacteria [96]. As no cytosolic homolog of Hsp100 has been identified so far in higher eukaryotes [80], transient and dynamic association but not irreversible sequestration of Hsp70 observed with SOD1 and polyglutamine aggregates suggests that at least in mammalian cells Hsp70 may on its own undertake a limited disaggregating function [67, 97]. Taken together, molecular chaperones and Hsp70 in particular orchestrate an intricate coordination between repair, deposition and elimination of misfolded and aggregated proteins through interconnected refolding, resolubilization and proteolytic degradation pathways, and thereby lie at the heart of maintenance of cellular proteostasis (Fig. 3).

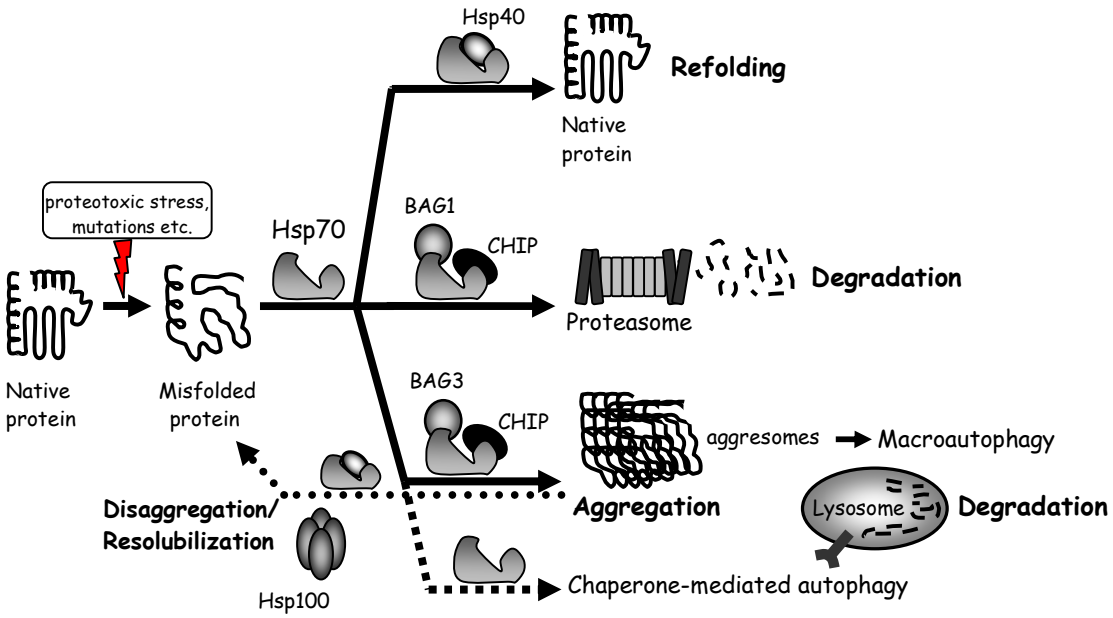

Figure 3. Cellular fates of misfolded proteins and defense mechanisms against protein aggregation. Misfolded proteins are recognized by molecular chaperones and can be refolded back to their native state by Hsp70 in concert with its co-chaperone Hsp40. Should this attempt of refolding fail, Hsp70 changes its partners to CHIP and BAG1, which together act to target the misfolded proteins for proteolytic degradation by the proteasome. When the proteasome is inhibited or its capacity is overwhelmed, Hsp70 switches its co-chaperone from BAG1 to BAG3, and directs misfolded proteins in a microtubule-dependent manner to aggresomes, which can later be degraded by lysosomal macroautophagy pathway. As a more specialized degradation route, some misfolded substrate proteins can also be targeted to lysosomes in a sequence-specific manner by Hsp70, which is known as chaperone-mediated autophagy (CMA). Finally, although to a limited extent in higher eukaryotes, molecular chaperones can also interact dynamically with the aggregates to resolubilize them for a second decision between refolding and degradation. (modified from refs. [80, 84, 92])

Given their central role in protection against protein misfolding and aggregation, levels of molecular chaperones are substantially increased in cells under proteotoxic stress conditions, such as elevation of temperature (i.e. heat shock) via a highly conserved adaptational response known as the heat shock response (HSR) [7] (Fig. 4). HSR is considered to be the prime sensor of abnormal, misfolded proteins accumulating in the cytosol [98] and is transcriptionally activated by heat shock factor 1 (HSF1) through a negative autoregulatory feedback mechanism [99]. HSF1, which is maintained under normal conditions as an inert monomer in an inhibitory complex with Hsp90, Hsp70 and

Hsp40, is set free upon stress where increased levels of damaged, misfolded proteins titrate the chaperones away from HSF1, allowing its trimerization, nuclear translocation and transcriptional activation of its target heat shock genes [100] (Fig. 4). Accordingly, expression of neurodegenerative disease-associated amyloid-β and expanded polyglutamine proteins activates the heat shock response in neuronal cells with a rapid and marked induction of Hsp70 [101-102]. However, induction of the HSR after heat shock is particularly deficient in primary hippocampal and motor neurons due to a lack of HSF1 expression [103] or a defect in HSF1 activation [104], respectively, which may in part explain the underlying basis for selective neuronal vulnerability to proteotoxic stress and neuron-specific aggregation of neurodegenerative disease proteins despite their broader patterns of expression [105].

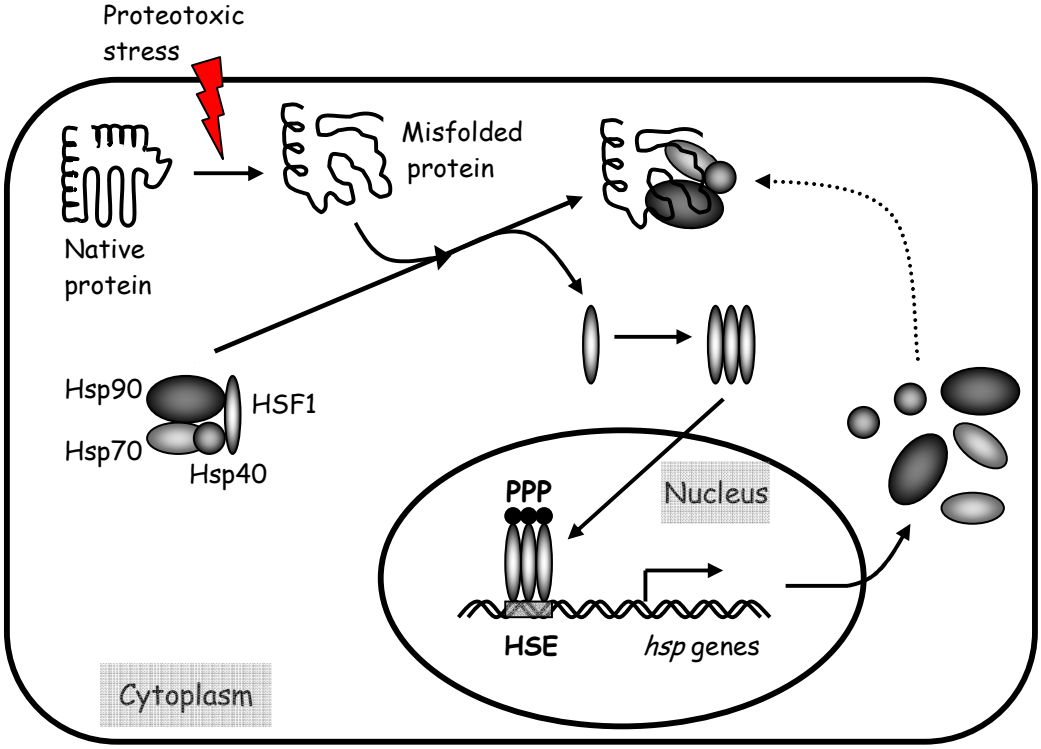

Figure 4. Induction of the heat shock response (HSR) by transcriptional activation of HSF1. Under normal conditions HSF1 is maintained as an inactive monomer in a complex with Hsp90, Hsp70 and Hsp40. Upon proteotoxic stress, increasing amounts of misfolded proteins titrate the chaperones away, setting HSF1 monomers free for trimerization. HSF1 trimers then translocate to the nucleus where they bind to heat shock elements (HSEs) in the promoters of heat shock genes. Following phosphorylation (**P**), HSF1 trimers acquire complete transcriptional activity that ultimately results in robust induction of a variety of heat shock proteins [99-100].

Endogenous levels of chaperones do not follow a consistent pattern of change in brains affected by neurodegenerative diseases [106] and no specific genetic mutation of chaperones has been identified so far for major amyloid-related diseases of neurodegeneration [107]. Hence, a decline in chaperone activity and capacity (i.e. chaperone overload) due to increasing amounts of a mutant, aggregation-prone protein has been proposed as another possible cause for disease pathogenesis [108]. Supporting this hypothesis, polyglutamine aggregates have been shown to disrupt protein folding homeostasis in *C. elegans*, causing induced aggregation of an otherwise soluble protein [109]. Moreover, chronic expression of an expanded polyQ protein in the presence of different temperature-sensitive mutant proteins was shown to induce the appearance of mutant phenotypes in *C. elegans* even at the permissive temperature, and vice versa, misfolded temperature-sensitive mutant proteins enhanced polyQ aggregation under normal physiological conditions [110]. Similarly, introduction of such destabilizing temperature-sensitive mutations into the genetic background of *C. elegans* was reported to strongly enhance the toxicity of mutant SOD1 aggregates, which were before only mildly toxic on their own, leading in turn to the exposure of deleterious phenotypes at permissive conditions [111]. Taken together, these studies suggest that cells have a limited overall folding capacity and when this capacity is overwhelmed by a severe aggregation-prone protein, as observed in neurodegenerative diseases, mild folding variants (i.e. destabilized polymorphic variants, harmless mutants) that are normally buffered and kept silent by chaperones may lose their folding assistance and become phenotypically exposed, leading to dysfunction in a diverse set of cellular pathways and thereby contributing to disease pathogenesis by yet an additional mechanism of cytotoxicity other than those mediated directly by the misfolded mutant protein (Fig. 2, see Section 1.3). Given the extensive and unique prevalence of single nucleotide polymorphisms (SNPs) in the human genome [112], 25%-30% of which are predicted to negatively affect protein stability or folding [113], this model can also help explain the high degree of variability observed in disease onset and progression [108, 110-111].

Not surprisingly, increased chaperone expression by genetic or chemical means has been extensively shown to suppress protein aggregation-induced toxicity in many cell culture

and animal models of neurodegenerative disease [114]. Although the effect of chaperones on the formation of inclusion bodies is highly variable, with the number/size of aggregates being decreased [56, 102, 109, 115-120], increased [116, 121-123] or remaining unchanged [118, 121-122, 124-126] with respect to the cell type [121], organism [127-128] and the specific members of chaperone families [116, 127-128] investigated, suppression of neurotoxicity and amelioration of disease phenotype is a universal feature of these proteins. To name a few, overexpression of cytosolic Hsp70 rescues primary neurons from toxicity induced by intracellular accumulation of amyloid-β, possibly by stimulating its ER-associated degradation [101]. Using a *Drosophila* model of spinocerebellar ataxia type 3 (SCA3) disease, directed expression of human Hsp70 was shown to suppress polyglutamine (ataxin-3-Q78)-induced neurodegeneration both in the eye and the nervous system, whereas an ATPase-deficient dominant-negative form of fly Hsp70 enhanced the disease pathology [124]. *Drosophila* homolog of Hsp40 alone could also reverse the degenerative eye phenotype in this model; however, when expressed together with Hsp70, there was a remarkable synergy in suppression of neurotoxicity, underlining the well characterized cooperation between these two chaperones [129]. Similarly, overexpression of inducible Hsp70 in SCA1 transgenic mice, which express ataxin-1 with 82 polyQ repeats (ataxin-1-Q82), improved behavioral and neuropathological phenotypes in a dose-dependent manner, with mice homozygous for Hsp70 showing a more robust improvement than hemizygous mice [118]. Supporting evidence for a neuroprotective role of Hsp70 in a non-polyQ animal model came from a *Drosophila* model of Parkinson's disease, in which directed expression of human Hsp70 prevented α-synuclein-induced dopaminergic neuronal loss, whereas interference with endogenous chaperone activity by a dominant-negative form of fly Hsp70 accelerated the neurodegenerative phenotype [126]. Furthermore, active HSF1 overexpression had a strong inhibitory effect on polyglutamine aggregate formation in a mouse model of Huntington's disease, and in cell culture this effect was found to be significantly higher than that observed by any combination of Hsp-s, indicating that HSF1 might protect through a systemic induction of the molecular chaperone network and/or induction of other, yet unknown, genes [130]. Consistent with these results, pharmacological induction of the heat shock response by the Hsp90-inhibitor geldanamycin [131], and

other small molecule drugs has been shown to delay or prevent the progression of neurodegenerative disease in different animal models [132-134].

Although generic cytoprotective functions of chaperones in maintaining proteostasis in the face of protein misfolding are well established as been described above, specific mechanisms underlying chaperone-mediated protection from toxicity with regard to distinct neurodegenerative disease-associated proteins have only been recently studied. For example, the Hsp70-Hsp40 chaperone system has been shown to inhibit *in vitro* self-assembly of prefibrillar oligomers of polyglutamine [135], α-synuclein [136] and amyloid-β [137] into mature amyloid fibrils by specifically binding to these early toxic species, which may likely serve *in vivo* to prevent their aberrant, cytotoxic interactions with other essential cellular components such as transcription factors [53], the proteasome and the plasma membrane (discussed in Section 1.3). In addition, overexpression of Hsp70 and/or Hsp40 in yeast [135] and mammalian cells [138] was shown to inhibit the formation of detergent-insoluble fibrillar polyQ (expanded huntingtin) aggregates, promoting instead the accumulation of amorphous, detergent-soluble aggregates. Remarkably, both detergent-insoluble and chaperone-favored detergent-soluble aggregates look morphologically similar under light/fluorescence microscope, complicating the interpretation of chaperone effect on protein aggregation in many studies [139]. Increased detergent-solubility of inclusion bodies by Hsp70 and Hsp40 overexpression was further confirmed in a *Drosophila* model of polyQ (ataxin-3-Q78) disease, and correlated well with a concomitant decrease in neurotoxicity observed [129]. Additional support for chaperone-mediated ultrastructural alterations in biochemical/physical state of aggregates has come from a mouse model of Parkinson's disease, where mice overexpressing Hsp70 had a significant reduction in their high molecular weight, detergent-insoluble α-synuclein levels [120]. Interestingly, in a cellular model of another polyQ disease, Hsp70-Hsp40 overexpression not only enhanced the solubility of expanded polyQ proteins, but also increased their degradation through the 26S proteasome, indicating that amorphous soluble aggregates favored by an excess of molecular chaperones are more efficiently turned over by the cell's proteolytic machinery in comparison to the insoluble fibrillar aggregates, and might contribute to chaperone

suppression of neurotoxicity [140]. In a similar line to this study, Hsp70, when overexpressed together with CHIP, was shown to protect from amyloid-β-induced toxicity by directly interacting with and promoting degradation of, amyloid-β in a proteasome-dependent manner in neuronal cells [141].

Neuroprotective mechanisms employed by molecular chaperones may not be exclusively limited to their direct effects on protein aggregation, but can also involve suppression of downstream events leading to neuronal apoptosis. For example, Hsp70 can inhibit mutant huntingtin-mediated activation of pro-apoptotic factors caspase-3 and caspase-9, thereby suppress apoptosis and protect against cellular toxicity, independently of its effect on polyQ aggregation [142]. Moreover, Hsp70 is a well-known suppressor of the stress kinase JNK whose activation promotes stress-induced apoptosis upon various protein-damaging conditions including heat shock [143-145]. Interestingly, expression of expanded polyQ proteins has been reported to induce a similar stress signal and lead to JNK-dependent apoptosis in neuronal cell lines, raising the possibility that inhibition of JNK activation might represent another mechanism by which Hsp70 can confer protection against polyQ-induced neurotoxicity [146-147].

1.4.2. Proteolytic degradation systems as a defense mechanism against aggregation

In addition to molecular chaperones, the cell's two main protein degradation systems, namely the UPS and macroautophagy, play essential roles in cellular defense against protein misfolding and aggregation (Fig. 3). Accordingly, many neurodegenerative disease-associated proteins including amyloid-β [148], tau [149], α-synuclein [150-151], mutant huntingtin [57, 121, 152-154], ataxin-1 [154-155], ataxin-3 [156] and SOD1 [157] have been extensively shown to be degraded by either the proteasome or macroautophagy or sometimes by both in a wide range of different cell culture studies, as mostly evidenced by increased accumulation of such proteins in the presence of specific inhibitors of these degradation machineries, suggesting a causative role for dysfunctional UPS and/or macroautophagy in the pathogenesis of neurodegenerative disorders. Indeed,

proteasome function has been reported to be impaired in the affected brain areas of patients with Alzheimer's and Parkinson's diseases [158-159]. Moreover, systemic exposure of rats to proteasome inhibitors [160] as well as targeted depletion of 26S proteasomes in mouse brain neurons [161] caused Parkinson's disease-like neurodegeneration in these animals. Loss of macroautophagy in mice was shown to lead to a severe neurodegenerative phenotype accompanied by an accumulation of polyubiquitylated inclusion bodies in neuronal cells [162-163]. Furthermore, induction of macroautophagy [164-165] and enhancement of proteasomal activity [166-169] by chemical or genetic means have been strongly associated with reduced toxicity in different cell culture and animal models of various neurodegenerative diseases. Probably, the strongest evidence for a causative role of dysfunctional UPS and macroautophagy in neurodegeneration has come from identification of mutations in the components of these degradation systems as the genetic defects responsible for hereditary/familial forms of several neurodegenerative disorders [170-171].

It has recently become more clear that there seems to be a coordination between these two degradation systems in elimination of misfolded and aggregated proteins that becomes even more critical in times of cellular stress [171-172]. Under normal conditions, soluble, monomeric misfolded proteins are preferentially degraded by the 26S proteasome [173]. However, when the UPS is functionally inhibited by proteasome inhibitors or its capacity is overwhelmed by an excess amount of misfolded proteins (i.e. UPS overload), as occurs experimentally with overexpression of the mutant protein from a high-copy plasmid in many cell culture studies [174], ubiquitylated misfolded proteins accumulate and are actively transported to cytoplasmic, juxtanuclear aggresomes [9, 57] (Fig. 3). Aggresomes are highly insoluble structures and incomparably large in size, thus cannot be accessed by the proteasome. In support of this argument, it has been shown that once captured into aggregates, misfolded proteins become virtually resistant to degradation by the proteasome [175]. In addition, as has been discussed in Section 1.3, the process of aggregation *per se* can even be inhibitory for the UPS function [63]. In light of these findings, a role for the ubiquitin-proteasome system in the clearance of pre-existing aggregates has largely been discredited, at least, as long as there is a continuous

production of misfolded proteins in cells [80]. Interestingly, if the production of such abnormal proteins ceases, as achieved by turning off the expression of mutant huntingtin in a conditional mouse model of Huntington's disease, intranuclear aggregates disappear in a proteasome-dependent manner, accompanied by a recovery of the behavioral disease phenotype [176-177]. However, in contrast to nuclear aggregates, cytoplasmic polyglutamine aggregates are efficiently cleared by macroautophagy [154]. Indeed, upon impairment of the UPS, macroautophagy has been shown to be induced as a compensatory degradation system, and plays a critical role in the removal of aggresomes [178-180]. Taken together, increasing evidence suggests that the UPS and macroautophagy work in coordination for the elimination of misfolded and aggregated proteins, but how and when the decision of degradation between these two major proteolytic pathways is made for a particular aggregation-prone protein in a given cellular context remains still largely unknown [171]. Several factors that are likely to have an influence on this decision seem to include intrinsic tendency of the mutant protein to aggregate, its cellular localization, its ubiquitylation status, and the type of proteotoxic stress the cell is under [171, 181].

1.5. Protein misfolding and proteostasis during aging

1.5.1. Protein misfolding during aging

Aging is characterized by a progressive accumulation of damage thought to be mainly induced by reactive oxygen and nitrogen species generated by increased oxidative stress as well as by glycation and cross-linking of proteins by glucose and other more reactive nutritional metabolites such as methyglyoxal [4, 182]. Although cells possess a number of different antioxidant enzymes to prevent the build-up of reactive oxygen species (ROS) such as superoxide dismutase, catalase, glutathione peroxidase and glutathione reductase, oxidative stress arises when concentrations of ROS exceed the cellular capacity to remove ROS, which ultimately results in widespread oxidation of

macromolecules including proteins [4]. Oxidized protein levels increase exponentially with aging of all animal species as mostly manifested by accumulation of reactive protein carbonyl groups, which is widely used as a cumulative measure of damage induced by multiple forms of ROS [5, 183]. Only some of these modifications to proteins can be reversed by specialized enzymes such as methionine sulfoxide reductases and thioltransferases, regenerating methionines and cysteines, respectively, while the majority of glycoxidative modifications are irreparable [182]. Irreversibly damaged proteins are recognized by chaperones, and targeted for proteasomal and lysosomal degradation pathways [184-185]. Apart from oxidation and glycation, other posttranslational modifications such as racemization and isomerization of certain amino acid residues as well as deamidation of asparagine and glutamine residues may spontaneously occur during the lifetime of any protein [182]. Such modifications can challenge protein conformation and lead to tertiary structural alterations, severely compromising protein stability [4]. Accumulation of damage by these posttranslational modifications in the course of aging is thought to result in destabilization and misfolding of the native protein form and promote aggregation in an environment where proteostatic defense mechanisms gradually decline [186].

1.5.2. Progressive decline of proteostasis during aging

Aging can be considered as a chronic form of proteotoxic stress accompanied by a progressive decline in the cellular capacity of the above-described major quality control systems (see Section 1.4) to cope with the damaged and/or mutant abnormal proteins, which may help explain why many neurodegenerative diseases are associated with old age [7, 78]. In this regard, collapse of folding capacity has been shown to represent an early molecular event in *C. elegans* aging, as evidenced by an age-dependent misfolding/aggregation and a loss of function of diverse temperature-sensitive mutant proteins even at the permissive condition, which coincides with a severely reduced activation of the heat shock response [187]. Indeed, attenuation of the heat shock response with diminished induction of chaperones as a result of impaired HSF1 activation

has been extensively reported in different tissues of various aged organisms [188-189]. Furthermore, chaperone functions are known to decline in aged hepatocytes of rats and in senile human lenses [188, 190]. Importantly, a direct effect of HSF1 on longevity has been shown in *C. elegans* where HSF1 is required to extend the lifespan of classical long-lived mutants deficient in insulin-like signaling, connecting the nutritional state and longevity with stress response [116, 191].

Additionally, the activities of protein degradation systems including the proteasome [192-193], macroautophagy [194] and chaperone-mediated autophagy [195] are all known to decline with aging, further compromising the overall capacity of the cellular quality control mechanisms. Age-dependent increase in oxidized, cross-linked proteins has been shown to exert a direct inhibitory effect on proteasome activity [193, 196]. The decline in proteasome activity with age is further supported by decreased subunit expression, alterations and/or replacement of proteasome subunits, impaired proteasome assembly and compromised protection of the proteasome by chaperones [192, 197-199]. Accumulation of lipid-protein cross-links in the form of the so-called age pigment lipofuscin may impair lysosomal macroautophagy during aging, which has been proposed to contribute to further ROS production via compromised turnover of dysfunctional mitochondria [200-201]. Moreover, defects in the formation/clearance of autophagic vacuoles and in hormonal regulation of macroautophagy by the nutritional state can also account for the decreased rates of macroautophagy in aging [202-203]. Finally, age-related decline in chaperone-mediated autophagy (CMA) has been linked to decreased levels and altered dynamics and stability of the lysosomal membrane receptor for this degradation pathway [204-205].

In conclusion, aging is increasingly characterized by the accumulation of oxidized, glycated and cross-linked proteins, which is likely due to their increased production and/or decreased elimination [182]. Disruption of the delicate balance between damage and repair/disposal in the course of aging favors conditions for protein aggregation with deleterious consequences on viability of the cell/organism, which may account for age-dependent increases in protein aggregation not only in the context of specific

neurodegenerative disease-associated proteins including expanded polyglutamine [206-207], ataxin-1 [45], amyloid-β [208], α-synuclein [209] and SOD1 [210], but also in the absence of any disease condition [211]. Interestingly, widespread protein aggregation with increased insolubility of several hundred proteins has recently been shown as an inherent part of aging in *C. elegans* even in a non-disease setting [211], consistent with the notion that many normal proteins have the capacity to aggregate under suitable conditions [8, 20], which seem to be well exemplified *in vivo* by an aging cellular environment. It is noteworthy to highlight that this finding is mainly observed in the postmitotic compartment and these misfolded proteins are very distinct in primary structure and lack specific sequences observed in neurodegeneration [211].

1.6. Selecting proper models of protein misfolding

Although protein aggregation is strongly associated with toxicity in cellular and animal models of neurodegenerative diseases as discussed above in detail, the toxic gain-of-function in these studies cannot be completely isolated from a loss of physiological function of the specific disease protein upon aggregation [212]. Therefore, the exact contribution of misfolded protein structures *per se* to toxicity remains largely unknown. Furthermore, the detrimental effects of protein misfolding and aggregation are known to be highly pronounced particularly in post-mitotic, especially neuronal cells as they cannot dilute the potentially toxic species through cell division [114]. However, how the expression of a misfolded protein affects proteostasis in replicating cells remains still poorly understood. To specifically analyze the role of protein misfolding on cellular physiology in transformed mammalian cells, we used two unrelated, destabilized, non-native protein models devoid of specific cellular functions and interactors, as *bona fide* inert misfolded proteins, allowing us to exclude any possible interference on cell fate that may arise from loss of native function and isolate only the gain-of-function effect of misfolded ensembles.

Green fluorescent protein (GFP) from the jellyfish *Aequorea victoria* and the prokaryotic antibiotic resistance enzyme chloramphenicol acetyltransferase (CAT) are two widely used reporters in mammalian cells. A C-terminal fusion of GFP to an amphipathic 16-residue degron peptide (GFP-degron) has initially been used as a reporter of the UPS activity after stably expressed in HEK-293 cells [61]. This short degron peptide was later shown to convert GFP into an aggregation-prone protein in *C. elegans* as well as in transiently-transfected mammalian neurons and HEK-293 cells [213]. Chloramphenicol acetyltransferase (CAT) consists of 221 amino acid residues, in which a cysteine residue at position 214 stabilizes and anchors the C-terminal α-helix (aa. 200-214) to a hydrophobic pocket formed by amino acids at the N-terminal half of the polypeptide. Loss of this key residue in C-terminally truncated Δ9CAT disrupts stability, and results in loss of chloramphenicol resistance and total deposition of the mutant protein in inclusion bodies in *Escherichia coli* [214-215], yet the effect of this deletion on CAT folding in the eukaryotic cytosol has not been investigated so far.

Both GFP- and CAT-destabilized variants are almost identical to their wild-type counterparts in molecular weight and sequence, meaning no difference in costs of expression and degradation. Furthermore, as being widely used reporters in eukaryotic cells, neither GFP nor CAT has any high-affinity interactions with other eukaryotic proteins. Both GFP and CAT lack disease-associated sequences such as polyQ or polyA expansions, ruling out special mechanisms of cytotoxicity originating from sequence-specific interactions (see Section 1.3). Finally, both GFP and CAT are devoid of cellular function; hence, no functional benefit is lost upon their misfolding and aggregation. Eliminating the above-mentioned factors posits both GFP-degron and Δ9CAT as suitable models to study the effects confined to protein misfolding.

2. Objectives

The main purpose of this study was to elucidate the general impact of protein misfolding *per se* on cellular physiology in transformed proliferating mammalian cells. The specific aims were as follows:

1. To investigate the effects of misfolded proteins on the heat shock response, chaperone-mediated folding capacity, cell proliferation and survival under basal and stress conditions

2. To investigate how genetic upregulation of major stress-inducible defense mechanisms combats the challenge induced by protein misfolding

3. Materials and Methods

3.1. Constructs

pEGFP-C1 was obtained from Clontech Laboratories (BD Biosciences, San Jose, CA, USA). GFP-degron was a kind gift of Christopher Link (University of Colorado, Boulder, CO, USA). GFP-wtCAT was generated by cloning the PCR-amplified full-length CAT (pCAT3-Control vector; Promega, Madison, WI, USA) region into the *Bgl*II/*Pst*I sites of pEGFP-C1, using forward primer 5'-AAAGATCTATGGAGAAAAAAATCAC-3' and reverse primer 5'-AACTGCAGTTACGCCCCGC-3'. For GFP-Δ9CAT cloning, reverse primer was designed to omit sequences corresponding to last 9 C-terminal amino acids (5'-AACTGCAGTTACTGTTGTAATTC-3'). Expression plasmids were kind gifts of the following colleagues: His-cBSA, Richard Voellmy (University of Miami, Miami, FL, USA); GFP170*, Elizabeth Sztul (University of Alabama, Birmingham, AL, USA); Hsp70.1pr-luc, Rick Morimoto (Northwestern University, Evanston, IL, USA); HSF1-myc-His, Lea Sistonen (Åbo Akademi University, Turku, Finland); Hsp70-myc, Kerstin Bellmann (Heinrich-Heine University, Düsseldorf, Germany); SIRT6-Flag, Haim Cohen (Bar-Ilan University, Ramat-Gan, Israel). Wild-type and deacetylase-deficient (H363Y) SIRT1 were obtained from Addgene (Cambridge, MA, USA). CMV-β-galactosidase was purchased from Promega, and pTK-luc was provided by László Hunyady (Semmelweis University, Budapest, Hungary). All constructs were verified by DNA sequencing.

3.2. Cell culture and transfection

COS-7 cells (SV40-transformed African green monkey kidney fibroblast-like cell line, CRL-1651; American Type Culture Collection, Manassas, VA, USA) were cultured in Dulbecco's modified Eagle's medium (DMEM with 4.5 mg/ml glucose, Life Technologies-Invitrogen, Carlsbad, CA, USA), supplemented with 10% fetal bovine serum (FBS), 100 U/ml penicillin and 100 μg/ml streptomycin, and 2 mM L-glutamine in

a humidified incubator at 37°C with 5% CO_2. Cells were plated at a density of 2.8-3×10^4 cells/cm^2, 1 d before transfection. Transient transfections were performed by Lipofectamine LTX reagent (Invitrogen) with the indicated plasmids according to the manufacturer's guidelines at a total DNA (μg) to Lipofectamine (μl) ratio of 1:3. Cells were processed for analyses at 24 or 48 h post-transfection.

3.3. Purification of aggregates and Western blotting

Cells were lysed in 1% Triton X-100 in PBS with protease inhibitors (Complete; Roche, Mannheim, Germany) for 30 min at 4°C. After sonication on ice for 3×10 sec, the lysates were cold-centrifuged (4°C) at 12,500 *g* for 15 min, and supernatants (S) containing soluble proteins were transferred to new tubes. Detergent-insoluble pellets (P), containing aggregated proteins, were solubilized in urea buffer (2% SDS, 6 M urea, 30 mM TrisHCl, pH 7.6) in the same volume, by shaking at 600 rpm for 10 min at 50°C. Equal volumes of protein extracts from each fraction (S, P) were resolved by SDS-PAGE. Western blotting was performed by semi-dry transfer to nitrocellulose membrane (Bio-Rad, Hercules, CA, USA) in transfer buffer (25 mM Tris, 192 mM glycine, 20% (v/v) methanol) at 1 mA/cm^2 for 1 h in cold room. Following blocking in 5% (w/v) skim milk powder (Fluka, Buchs, Switzerland) in TBS-T (TBS with 0.1% (v/v) Tween-20; Bio-Rad) for 1 h at room temperature, blots were probed with antibodies against GFP (1:5000; kind gift of László Buday, ref. [216]), Hsp70 (HSPA1A/B; 1:2000, SPA-810; Stressgen, San Diego, CA, USA), HSF1 (1:1000, #4356; Cell Signaling Technology, Danvers, MA, USA), SIRT1 (1:1000, #2493; Cell Signaling Technology) and SIRT6 (1:1000, S4197; Sigma-Aldrich, St. Louis, MO, USA) in solutions containing 5% (w/v) BSA in TBS-T, overnight at 4°C. After washing with TBS-T buffer, blots were incubated in appropriate HRP-conjugated secondary antibodies (DakoCytomation, Glostrup, Denmark) in blocking solution for 45 min at room temperature. Immunodetection was performed by ECL (PerkinElmer, Wellesley, MA, USA).

3.4. Estimation of misfolded protein expression levels

Cells were trypsinized, split and the ratio of GFP-positive cells was determined by flow cytometry (FACSCalibur; BD Biosciences) using FL1 (530/30 BP) channel. The rest of the cells were lysed in urea buffer, and protein concentration was determined by detergent-compatible BCA protein assay (Pierce Biotechnology, Rockford, IL, USA). 10 μg of total protein extracts were loaded on SDS-PAGE along with a gradient of known quantities of recombinant GFP (rGFP; Roche). Based on the rGFP calibration curve, GFP protein amounts were estimated by densitometric analysis of the GFP Western blots using ImageJ (U. S. National Institutes of Health, Bethesda, MD, USA). After total protein amounts were normalized to their corresponding GFP-positive cell ratios, GFP expression levels were determined as a percentage of the total protein in GFP-positive cells.

3.5. Immunofluorescence microscopy

Cells were grown on poly-L-lysine-coated (0.1 mg/ml; Sigma) glass coverslips. At 2 d after transfection, cells were fixed and permeabilized in pre-chilled (-20°C) absolute methanol for 5 min. After being washed twice in PBS, cells were blocked in 1% (w/v) BSA in PBS for 1 h at room temperature, then incubated in an anti-Hsp70 mouse monoclonal antibody solution (1:100, #610608; BD Biosciences) recognizing both inducible (HSPA1A/B) and constitutive (HSPA8) Hsp70 for 1 h at room temperature. Following washing with PBS, cells were stained in Cy3-conjugated goat anti-mouse secondary antibody solution (1:500, #115-165-003; Jackson ImmunoResearch Labs, West Grove, PA, USA) for 30 min at room temperature. After washing, cells were counterstained with DAPI (0.1 μg/ml; Molecular Probes, Eugene, OR, USA) for 3 min. Coverslips were mounted using Vectashield mounting medium (Vector Laboratories, Burlingame, CA, USA) and visualized by an epifluorescence microscope (Eclipse E400; Nikon, Tokyo, Japan), employing a 10×100× (oil immersion) magnification with the appropriate filter-sets (DAPI: UV-1A, GFP: B-2A, Cy3: G-2A).

3.6. HSF1 transactivation and luciferase folding assays

For HSF1-dependent transactivation assay, cells were cotransfected with a reporter plasmid harboring the *hsp70* promoter region upstream of the firefly luciferase gene (hsp70.1pr-luc) and a β-galactosidase plasmid driven by the cytomegalovirus promoter (β-gal) as an internal control to correct for transfection and cell lysis efficiencies. For luciferase folding assay, a firefly luciferase plasmid harboring the thymidine kinase minimal promoter (TK-luc) was used instead. Cotransfections were done at a ratio of 4:1:1 (protein model: luc: β-gal). Cells were lysed in 1X Reporter Lysis Buffer (Promega) for 20 min at room temperature with occasional rocking. For luciferase folding assay, cells were immediately cooled on ice after heat shock (42°C) to prevent renaturation of luciferase, and cell lysis was performed on an ice bed for 40 min. Cells were then scraped off the wells, vortexed for 15 sec, and centrifuged (4°C) at 12,500 *g* for 3 min. Cell lysates were processed for β-galactosidase (Promega) and luciferase (Bright-Glo; Promega) assays according to the manufacturer's protocols. Absorbance at 420 nm and luminescence were measured by a multimode plate reader (Varioskan Flash; Thermo Scientific, Wiesbaden, Germany), respectively. Data were expressed after normalized by dividing luminescence values by β-gal activities (luc/β-gal).

3.7. BrdU incorporation

Cells grown on poly-L-lysine-coated (0.1 mg/ml; Sigma) glass coverslips were pulse-labeled with bromodeoxyuridine (BrdU; Molecular Probes) at 100 μM for the last 3 h of their transfection period. After being washed in PBS, cells were fixed at 4°C for 30 min in formaldehyde freshly prepared from 4% (w/v) paraformaldehyde (Sigma). Following washing in PBS containing 0.5% (w/v) BSA (wash buffer), cells were permeabilized in 1% Triton-X in PBS for 20 min at room temperature. As the subsequent step of HCl treatment would be destructive to the native GFP fluorescence, cells were stained at this stage with FITC-conjugated anti-GFP antibody (1:100, ab6662; Abcam, Cambridge, MA, USA) for 40 min at room temperature. Following washing, genomic DNA was denatured

in freshly prepared 2 M HCl containing 0.5% (v/v) Tween-20 (Bio-Rad) for 30 min at 37°C, in order to allow anti-BrdU antibody to gain access to the DNA, as the antibody can detect incorporated BrdU only in single-stranded (denatured) form. Cells were then stained with Alexa Fluor 546-conjugated anti-BrdU antibody (1:50, A21308; Molecular Probes) for 40 min at room temperature. Following multiple washes, cells were counterstained with DAPI (0.1 μg/ml; Molecular Probes) for 3 min, and analyzed by an epifluorescence microscope (DMI6000B; Leica Microsystems, Wetzlar, Germany), employing a 10×10× magnification with the appropriate filter-sets (DAPI: A4, FITC: L5, Alexa Fluor 546: TX2). Image analysis was performed by counting 600-700 cells/area for 6 different areas randomly selected from each sample.

3.8. Annexin assay

Cells were treated with the proteasome inhibitor MG-132 (2 μM; Calbiochem, San Diego, CA, USA) on the same day of transfection, for a total duration of 42 h. Cells were then trypsinized, pooled together with the cell supernatant, and cold-centrifuged (4°C) at 2000 rpm for 5 min. Following washing in ice-cold PBS, cells were resuspended in 100 μl annexin buffer (10 mM HEPES, 140 mM NaCl, 2.5 mM $CaCl_2$, pH 7.4) and stained with 5 μl annexin V-Alexa Fluor 647 conjugate (Molecular Probes) for 20 min at room temperature. After the incubation period, 900 μl of annexin buffer was added. Cells were then mixed gently, and immediately analyzed by flow cytometry (FACSCalibur; BD Biosciences). 10,000 cells were counted and gated in an FSC/SSC density plot to eliminate cell debris. Native GFP and annexin signals were measured in a dual-parameter density plot by FL1 (530/30 BP) vs. FL4 (661/16 BP) channels, respectively. Acquisition and analysis were done by BD CellQuest Pro software (BD Biosciences). The instrument settings were as follows: FSC=E-1 (log), SSC=235 V (log), FL1=405 V (log), FL4=345 V (log). The percentage of annexin-positive cells out of the GFP-positive subpopulation was calculated by the formula “UR/(UR+LR)×100”, as obtained from quadrant statistics.

3.9. Analysis of cellular DNA content

Cells were treated with 2 μM MG-132 (Calbiochem) 1 d after transfection for 20 h. For concomitant heat-stress experiments, one set of cells was heat-shocked at 43°C for 30 min in a circulating water bath, while another set was kept at 37°C. Cells were then harvested, pooled together with the cell supernatant and cold-centrifuged (4°C) at 1800 rpm for 3 min. The resulting cell pellet was resuspended in 1 ml pre-chilled (at -20°C) 70% ethanol at room temperature for 30 min, and then stored at -20°C overnight. Fixed cells were pelleted at 2200 rpm for 5 min at 4°C and resuspended in 1 ml extraction buffer (200 mM Na_2HPO_4, pH 7.8 adjusted with 200 mM citric acid) containing RNase A (10 μg/ml; Sigma). Following incubation at room temperature for 30 min to extract degraded, low molecular weight DNA fragments out of apoptotic cells, remaining nuclear DNA was stained by propidium iodide (PI, Sigma; 10 μg/ml) for 10 min at room temperature. Gated total cell population was immediately analyzed by a flow cytometer (FACSCalibur; BD Biosciences) in a dual-parameter density plot with FL1 (530/30 BP) vs. FL3 (650 LP) channels, measuring the native GFP and PI fluorescence, respectively. Acquisition and analysis were done by BD CellQuest Pro software (BD Biosciences). The instrument settings were as follows: FSC=E-1 (log), SSC=235 V (log), FL1=355 V (log), FL3=350 V (log). For data analysis, only the percentage of GFP-positive cells with an intact cell cycle (i.e. combination of G1-S-G2/M peaks) out of the gated total population (i.e. UR values obtained from the quadrant statistics) was taken into consideration.

3.10. Statistical analysis

Data were analyzed using the SPSS software 15.0 (SPSS Inc., Chicago, IL, USA) and compared by Student's *t* test. All data were presented as means ± S.E.M. of indicated number of independent experiments. Statistical significance was indicated as follows: n. s., non-significant, *$p<0.05$, ** $p<0.01$, *** $p<0.001$.

4. Results

4.1. GFP-degron and GFP-Δ9CAT display characteristics of misfolding

First, we generated GFP-fusions of wildtype CAT (wtCAT) and Δ9CAT to facilitate their visualization and detection. Along with GFP and GFP-degron, we used these GFP-tagged CAT variants to transiently transfect COS-7 cells, and investigated their solubility by sequential extraction into detergent-soluble and insoluble fractions. While GFP and GFP-wtCAT showed a relatively equal distribution between soluble (S) and pellet (P) fractions, GFP-degron and GFP-Δ9CAT sedimented predominantly in detergent-insoluble pellet fraction (Fig. 5A). This sedimentation was not due to a higher level of overexpression, since both mutants were detected at a level 2- to 5-fold less than their wild-type controls (see the sum of S+P fractions in Fig. 5A, and Fig. 6A). Moreover, we observed GFP-reactive bands at higher molecular weight in the pellet fractions of GFP-degron and GFP-Δ9CAT, indicating the presence of insoluble oligomeric and/or ubiquitylated species generated by these mutant proteins; both of which are characteristic of the exposure of buried reactive regions in misfolded ensembles [9, 78]. The GFP pellet showed a very weak GFP-reactivity at around 55 kDa, which may correspond to a dimer, i.e. a tendency to aggregate when strongly overexpressed, as reported earlier [213], however, it did not resemble to the multiple bands detected in GFP-degron and GFP-Δ9CAT pellets. Deletion of the 9 C-terminal amino acids also caused total loss of CAT enzymatic activity, as revealed by spectrophotometric CAT assay [217] (Fig. 5B). Thus, destabilizing modifications induced the loss of native conformation and converted both GFP and GFP-wtCAT into a less soluble state.

Next, to address whether the decreased solubility of GFP-degron and GFP-Δ9CAT proteins would be accompanied by changes in the morphological level, we examined their subcellular distribution under fluorescence microscopy by following the GFP signal. Both GFP-degron and GFP-Δ9CAT prevailed predominantly as intense deposits of perinuclear and juxtanuclear aggregates resembling aggresomes [9, 30, 218], while GFP and GFP-wtCAT were distributed diffusely in the cytoplasmic and nuclear compartments

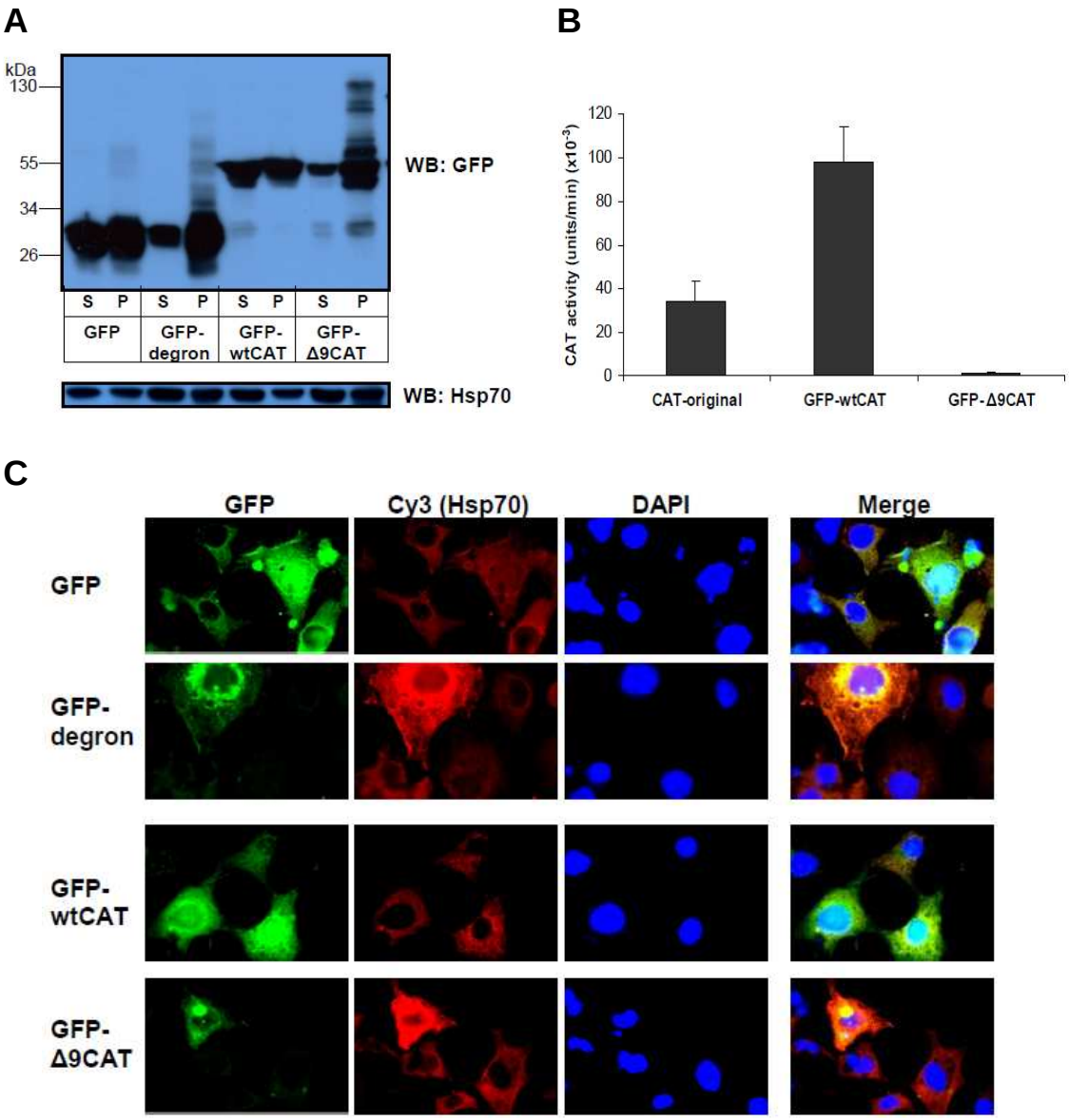

Figure 5. **GFP-degron and GFP-Δ9CAT display characteristics of misfolding. (A)** Misfolding GFP-degron and GFP-Δ9CAT proteins sediment in detergent-insoluble aggregates and increase Hsp70 (HSPA1A/B) protein level. After transient transfections with the indicated constructs (GFP, GFP-degron, GFP-wtCAT, GFP-Δ9CAT), COS-7 cells were lysed and cell lysates were separated into soluble (S) and detergent-insoluble pellet (P) fractions by centrifugation, and analyzed by Western blotting for GFP and Hsp70. Images are representatives of 5 independent experiments. **(B)** GFP-Δ9CAT does not exhibit detectable enzymatic activity. Lysates from original CAT (Promega), GFP-wtCAT and GFP-Δ9CAT-transfected cells were mixed with CAT reaction buffer (0.1 mM acetyl-CoA, 0.4 mg/ml DTNB, 0.1 M Tris-HCl, pH 7.8) and absorbance at 414 nm was measured for 5 min at 23 sec intervals. Chloramphenicol is then added at 0.1 mM and absorbance is followed for another 5 min. Slopes of the recorded data were converted into enzyme activity units. Data represent means ± S.E.M. of 2 independent experiments. **(C)** Misfolding proteins form perinuclear aggregates and accumulate total Hsp70 protein *in vivo*. Transfected cells grown on coverslips were fixed in methanol, stained by an antibody recognizing both inducible (HSPA1A/B) and constitutive (HSPA8) Hsp70 followed by a Cy3-conjugated secondary antibody and DAPI for nuclear DNA, and were visualized under a fluorescence microscope. Images are representatives of 5 independent experiments.

(Fig. 5C). These observations were also confirmed in live cells (data not shown) and demonstrated that the decreased solubility was not an artifact caused by cell lysis, but was rather due to the formation of aggregated ensembles inside living cells, a hallmark of protein misfolding [8]. Our findings on the perinuclear deposition of GFP-degron in mammalian cells are consistent with those reported by Link *et al*. [213].

Expression of both GFP-degron and GFP-Δ9CAT increased the level of inducible Hsp70 (HSPA1A/B) (Fig. 5A, bottom panel). Equally increased Hsp70 levels were observed in the soluble and pellet fractions, respectively, of both mutants, indicating that Hsp70 did not show a strong preference toward insoluble species after cell lysis. Moreover, immunofluorescence analyses showed that GFP-degron and GFP-Δ9CAT led to a robust accumulation of constitutive and inducible Hsp70 (HSPA8 and HSPA1A/B, respectively) only in cells where they were expressed, in contrast to the soluble controls GFP and GFP-wtCAT whose Hsp70 levels stayed comparable to the neighboring untransfected cells of GFP-degron and GFP-Δ9CAT samples (Fig. 5C). Remarkably, Hsp70 was strongly enriched in both GFP-degron and GFP-Δ9CAT aggregates. The Western blot and immunofluorescence data together suggest a transient association of Hsp70 with the misfolded/aggregated species of GFP-degron and GFP-Δ9CAT, and are consistent with previous reports showing dynamic interaction of Hsp70 with polyglutamine [97] and SOD1 [67] aggregates. These results demonstrate that both GFP-degron and GFP-Δ9CAT exhibit decreased solubility and aggregation, induce and transiently associate with the chaperone Hsp70, establishing both GFP-degron and GFP-Δ9CAT as *bona fide* misfolded proteins.

4.2. Misfolded proteins undergo proteasomal degradation

Both Link *et al.* [213] and we observed GFP-degron as perinuclear aggregates (Fig. 5) though GFP-degron-positive cells were always only a modest fraction (5-15%) of the total cell population. Based on the notion that proteolytic degradation pathways constitute an essential part of the cellular defense mechanisms against protein misfolding and

aggregation as been discussed in Section 1.4.2, we tested whether a proteolytic degradation of misfolded proteins occurred. Using the proteasome inhibitor, MG-132, we detected an increased level of both GFP-degron and GFP-Δ9CAT, as demonstrated by flow cytometry (Fig. 6A). MG-132, when applied at a concentration as low as 2 μM (a concentration without severe cytotoxicity) for 20 h, induced a significant increase in GFP-degron- and GFP-Δ9CAT-positive cells, approaching the ratio of GFP- and GFP-wtCAT-positive cells. The stabilization of misfolded proteins by MG-132 reached a plateau already at 2 μM, and any higher concentration did not result in a further increase in GFP-positivity. It is important to note that neither GFP-degron nor GFP-Δ9CAT was detected in soluble forms, and proteasome inhibition did not significantly change the appearance and topology of aggregates examined by fluorescence microscopy, which suggests that aggregation is a direct consequence of the presence of misfolded, undegradable ensembles. We also found that 3-methyladenine (3-MA), a specific inhibitor of macroautophagy, did not increase GFP-fluorescence when applied alone or in combination with MG-132 (Fig. 6B), ruling out any involvement of macroautophagy in the clearance of GFP-degron, as well as suggesting that the stabilization observed with MG-132 was not due to an unspecific inhibition of the cellular proteolytic capacity. Altogether, these results define the proteasome responsible for the degradation of these misfolded proteins.

Flow cytometric histograms of MG-132-treated (5 μM, 20 h) cell populations show that proteasome inhibition stabilizes GFP-degron and GFP-Δ9CAT at fluorescence intensities exceeding 10^2 and 3×10^2, respectively, suggesting misfolded species are tolerated below these thresholds (Fig. 6C). Using a recombinant GFP (rGFP) calibration curve, we determined the corresponding expression levels by densitometric analysis of anti-GFP Western blots of total cell lysates whose amount (10 μg) was normalized to the corresponding GFP-positive cell ratios (Fig. 6D and E). While traces of misfolded proteins were detected using these settings, inhibition of their turnover increased the average expression of GFP-degron and GFP-Δ9CAT to 2.2 *vs.* 0.9% of total cellular protein, respectively. These results are consistent with the higher peak of GFP-degron observed in flow cytometry (Fig. 6C). Considering the logarithmic scale of fluorescence

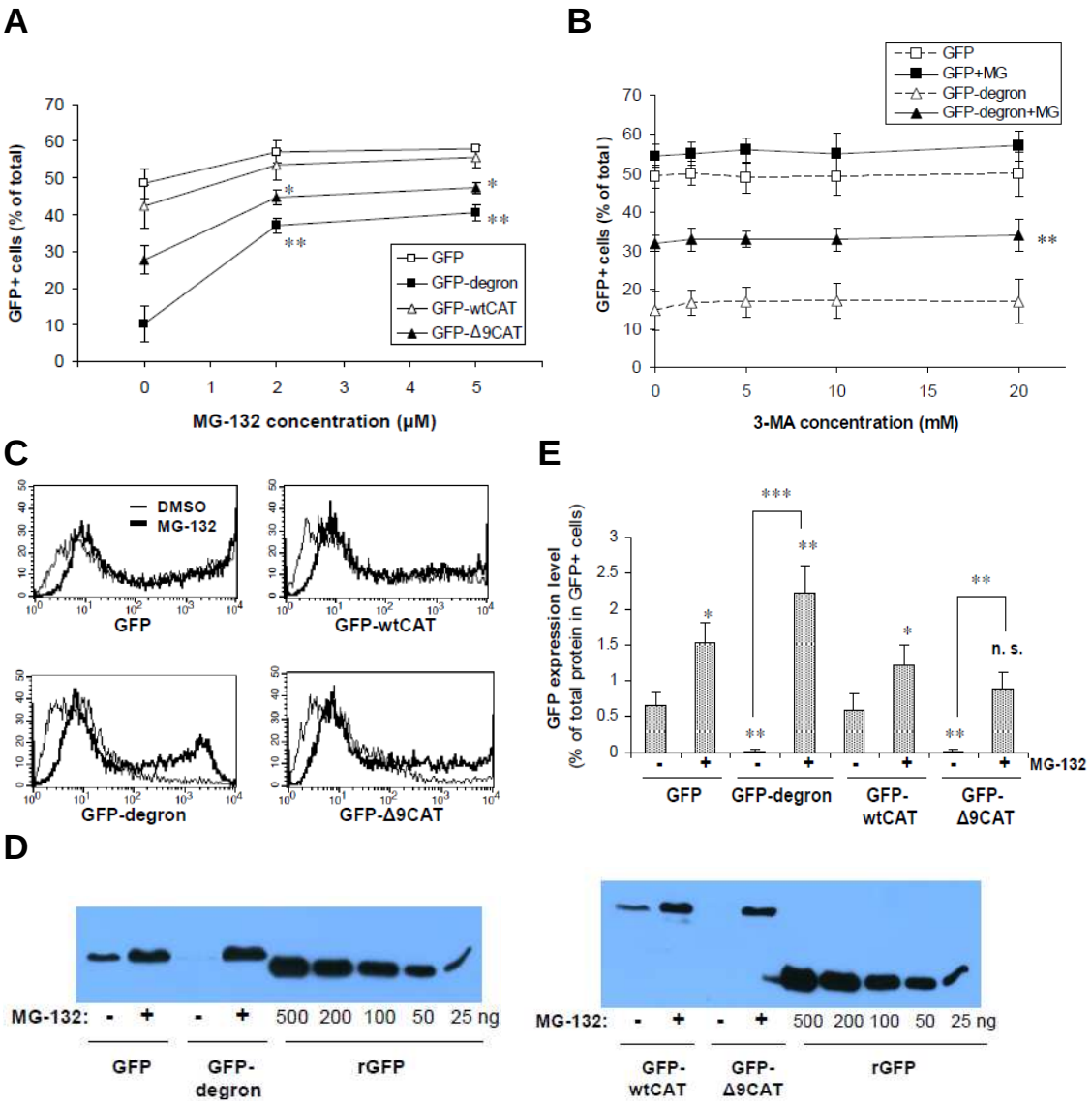

Figure 6. Misfolded proteins undergo proteasomal degradation. (A) Cells were treated with increasing concentrations of the proteasome inhibitor MG-132 for 20 h before they were harvested and analyzed by flow cytometry. Chart shows the percentage of GFP-positive cells in total cell population. Data represent means ± S.E.M. of 3 independent experiments and were compared to their own untreated control samples in the absence of MG-132. **(B)** GFP-degron is not degraded by macroautophagy. Cells were treated with increasing concentrations of 3-MA for 20 h in the absence and presence of MG-132 (2 μM) before they were harvested and analyzed by flow cytometry. Data represent means ± S.E.M. of 2 independent experiments. Significance indicated represents comparison between all respective data points of GFP-degron with and without MG-132 treatment. **(C)** Cells, treated with or without MG-132 (5 μM, 20 h), were harvested and analyzed by flow cytometry. Histogram overlays show MG-132-treated (thick line) and untreated (thin line) cell populations for each protein model as a function of GFP fluorescence intensity. Images are representatives of 2 independent experiments. **(D)** Western blot analysis for GFP of total protein extracts (10 μg) of cells from C, using a recombinant GFP (rGFP) calibration. Images are representatives of 2 independent experiments. **(E)** GFP expression levels. Densitometric analysis of Western blots from D, normalized to their corresponding GFP positivities. Data represent means ± S.E.M. of 2 independent experiments and were compared to untreated GFP and GFP-wtCAT controls (asterisks on columns) and to GFP-degron/GFP-Δ9CAT in the absence or presence of MG-132, respectively (linked bars).

and the abovementioned thresholds, we assume that maximal expression levels cannot exceed 1% to 2% of total cellular proteins, and that misfolded proteins in the range of approximately 0.02% to 0.04% of total cellular proteins are efficiently sensed and disposed.

4.3. Misfolded proteins activate the *hsp70* promoter

Since we could see an accumulation of Hsp70 protein with both misfolded proteins (Fig. 5A and C), we were interested whether they would induce transcriptional activation (transactivation) of heat shock factor 1 (HSF1), responsible for the induction of *hsp* genes [99-100]. To accomplish this, we took use of a reporter construct harboring the *hsp70* promoter fused to firefly luciferase [219]. GFP-degron expression resulted in a moderate induction of the reporter at 37°C by up to 4-fold compared to that of GFP (Fig. 7A). GFP-Δ9CAT was able to induce the reporter gene at a smaller, comparable extent (3-fold increase compared to the induction by GFP-wtCAT). Induction of the reporter by misfolded proteins was completely blunted by cotransfection with HSF1 siRNA (data not shown), confirming that the induction was entirely HSF1-dependent, consistent with previous results [100, 220]. Using a construct harboring the endoplasmic reticulum chaperone *grp78* promoter fused to firefly luciferase, we did not detect an activation of the *grp78* promoter by GFP-degron and GFP-Δ9CAT (data not shown), suggesting that misfolding of cytosolic proteins does not result in the activation of the endoplasmic reticulum (ER) unfolded protein response (UPR), consistent with recent studies in yeast [221-222].

We next addressed how misfolded proteins would interfere with the induction of the heat shock response (HSR) by a moderate proteotoxic heat stress (43°C, 30 min). The presence of GFP-degron and GFP-Δ9CAT, neither failed to synergize with, nor compromised the heat-induced activity of the reporter gene construct, respectively, suggesting that the induction of the heat shock response was not significantly changed by a transient expression of a single misfolded protein (Fig. 7B).

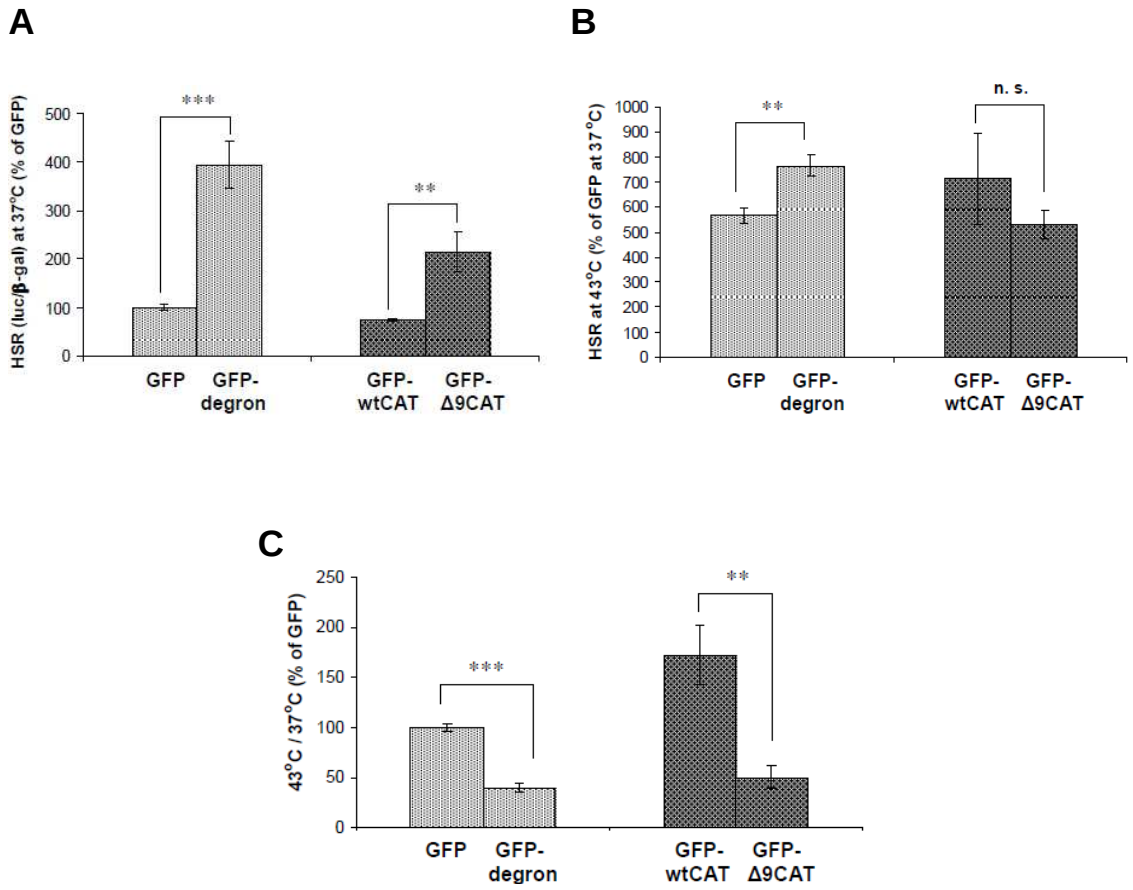

Figure 7. Misfolded proteins activate the *hsp70* promoter. HSF1-transactivation at 37°C (A), heat-induced HSF1-transactivation (B), and the ratio of induced and basal outputs (C). **(A, B)** Along with the indicated constructs, cells were cotransfected with hsp70.1pr-luc and β-galactosidase (β-gal) plasmids. A second set (B) was given a heat shock at 43°C for 30 min. Luciferase and β-gal assays were performed 18 h later, and their ratios were expressed as percentages of the value obtained in the GFP sample. **(C)** Alternatively, fold inductions in the heat shock response were calculated by dividing the normalized (luc/β-gal) heat-shocked (43°C) values by their corresponding basal (37°C) values, and are displayed in the chart as a percentage of the value obtained in the GFP sample. Data represent means ± S.E.M. of 7 independent experiments for GFP and GFP-degron, and 3 independent experiments for GFP-wtCAT and GFP-Δ9CAT, respectively. Values were compared to the respective wild-type controls.

However, compared to their wild-type counterparts, misfolded proteins led to a higher basal level as well as a reduced reserve capacity of the heat shock response (i.e. decreased fold induction in the heat shock response, as calculated by dividing the response at 43°C by that of 37°C), suggesting that the induction of heat shock proteins was under a constant strain at basal conditions (Fig. 7C). We observed the same phenomenon with two other non-native misfolded protein models, namely GFP-cBSA

(bovine serum albumin lacking the peptide signal for ER targeting and misdirected to the cytosol, hence missing stabilizing disulfide bridges) and GFP170* (a fusion of GFP to an internal segment of the coiled-coil region of the Golgi complex protein 170, forming nuclear aggregates and colocalizing with Hsp70, also see Section 1.3), consistent with previous reports ([60, 220] and data not shown). Hence, we conclude that a transient expression of a single misfolded protein induces HSF1-dependent transactivation without a severe compromise of heat inducibility along with a reduced reserve capacity of the heat shock response.

4.4. Opposing effects by GFP-degron and GFP-Δ9CAT on chaperone-mediated folding

Chronic expression of polyglutamine proteins was previously shown to interfere with protein folding homeostasis [109-110] and to promote a loss of function of diverse proteins with destabilizing temperature-sensitive mutations in the postmitotic nematode *C. elegans* [110], as mentioned before in Section 1.4.1. To test this possibility in replicative cells, we asked how acute expression of misfolded proteins would affect the activity of firefly luciferase, a metastable multidomain protein commonly used as a model substrate to monitor chaperone activity/function [223]. Overexpression of GFP-degron caused a 25% decrease of luciferase activity compared to that of wildtype GFP-cotransfected cells at 37°C (Fig. 8A). Surprisingly, GFP-Δ9CAT enhanced luciferase activity by 20% compared to that of GFP-wtCAT at 37°C (Fig. 8B). With increasing periods of time at heat shock (42°C), the difference between luciferase activities of both GFP *vs.* GFP-degron and GFP-wtCAT *vs.* GFP-Δ9CAT pairs disappeared, suggesting that increasing amounts of denatured proteins override the effect of a single misfolded protein. Similar phenomena were observed with MG-132 (2 μM, 20 h), consistent with the proteasomal clearance of an extensive amount of mistranslated/misfolded proteins already at non-stress conditions [224]. Hsp70 overexpression promoted luciferase folding by about 25% for all constructs even in the presence of MG-132, establishing that global

manipulations of the proteostatic buffer are efficiently reflected in firefly luciferase folding (data not shown). None of the interventions affected the activity of β-galactosidase (data not shown). We conclude that in contrast to global proteotoxic stresses (heat shock and MG-132), short-term expression of single misfolded proteins exerts a modest effect on chaperone-mediated protein folding.

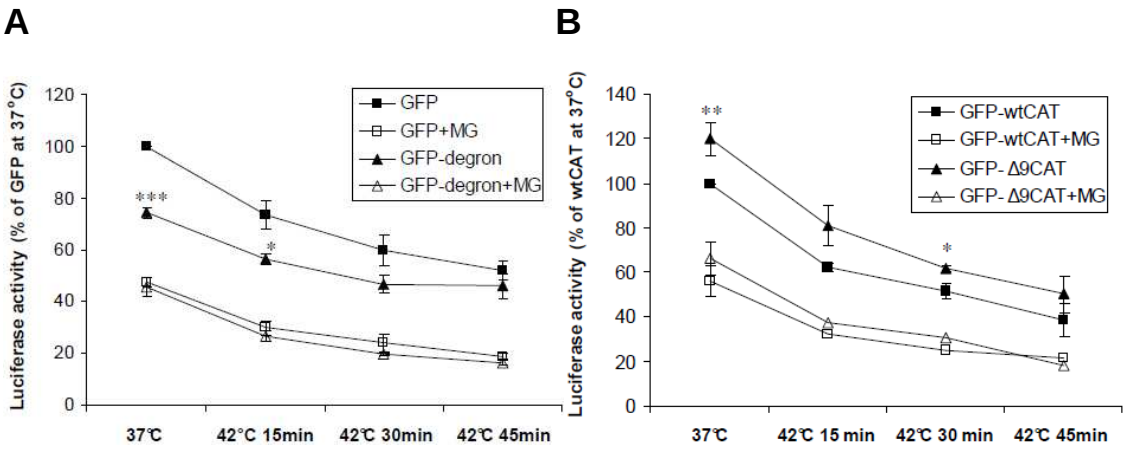

Figure 8. Opposing effects by GFP-degron and GFP-Δ9CAT on chaperone-mediated folding. GFP-degron compromises **(A)**, while GFP-Δ9CAT enhances **(B)** firefly luciferase folding at 37°C. Along with the indicated protein models, cells were cotransfected with TK-luc and β-gal plasmids. After treatment with or without MG-132 (2 μM, 20 h), cells were either incubated at 37°C or given a heat shock at 42°C for the indicated periods of time. Immediately after the heat shock, cells were cooled on ice, lysed and analyzed, as described in Materials and Methods. Charts show normalized luciferase (luc/β-gal) activities as a percentage of the value obtained in the respective wild-type controls at 37°C without MG-132 treatment. Data represent means ± S.E.M. of 3 independent experiments and were compared to the respective wild-type controls subjected to the same treatment.

4.5. Misfolded proteins inhibit cell proliferation

We next investigated the consequences of protein misfolding on cell proliferation, an essential property of the replicative compartment. Incorporation of the thymidine analog bromodeoxyuridine (BrdU) into genomic DNA during DNA replication (S phase) is a well-established indicator of cell division. After cells were pulse-labeled with BrdU at 100 μM for the last 3 h of their transfection periods, they were immunostained with both anti-GFP and anti-BrdU antibodies to enable differential analysis of rates of BrdU uptake in transfected and untransfected subpopulations, respectively (Fig. 9A). Image analyses and quantification of dual immunofluorescence data revealed that both GFP-degron- and GFP-Δ9CAT-positive cells incorporated less BrdU than their wild-type counterparts (Fig. 9B). Induction of cell proliferation arrest by misfolded proteins was more pronounced with GFP-degron, as only 2% of GFP-degron-positive cells were BrdU-positive, while for GFP-Δ9CAT BrdU positivity was about 11%, suggesting a stronger impact of GFP-degron on cell growth, in agreement with its more pronounced effects on cell physiology (cf. GFP-degron and GFP-Δ9CAT in Figs. 5-8). MG-132 (2 μM, 20 h) treatment completely blocked BrdU uptake in all cells regardless of their transfection status (data not shown), consistent with previous studies on other cell lines [225-226]. Thus, similarly to proteasome inhibition, misfolded proteins arrest cell proliferation.

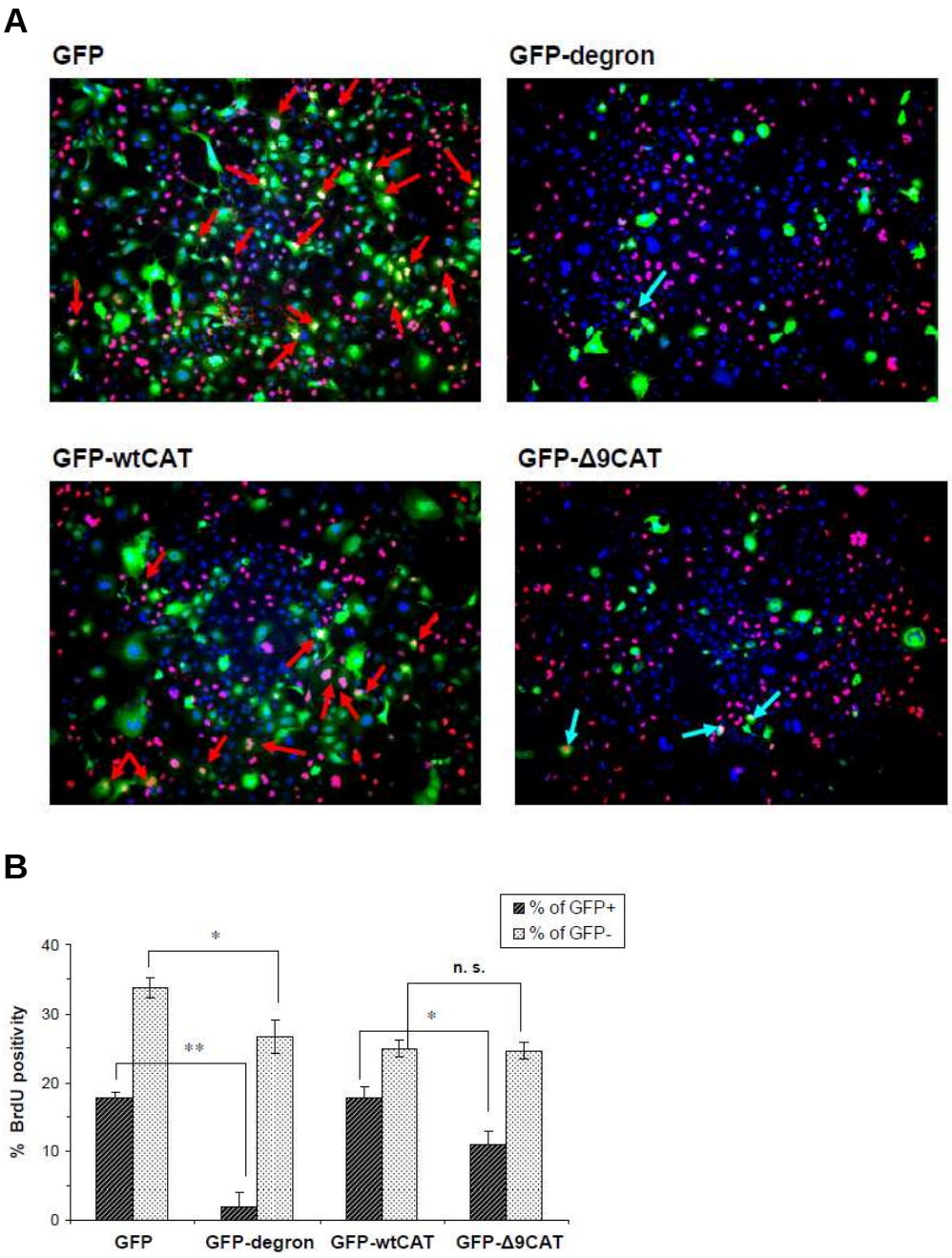

Figure 9. Misfolded proteins induce cell proliferation arrest. Transfected cells were pulse-labeled with BrdU (100 μM) for 3 h, fixed and immunostained with anti-GFP and anti-BrdU antibodies followed by a nuclear staining (DAPI). **(A)** Fluorescence microscopy pictures show merged images of GFP (green), BrdU (red) and nuclei (blue) stainings. Arrows indicate cells that are positively stained for both GFP and BrdU. Image for each construct is a representative of 12 different regions from 2 independent experiments. **(B)** Quantification of dual immunofluorescence data. 6 different areas randomly selected from each protein model with an average of 600-700 cells/area were first counted for single DAPI, GFP and BrdU signals. Double-positives for both GFP and BrdU signals were then counted, and calculations were done accordingly to determine percentages of BrdU positivity in GFP-positive (dark bars) and GFP-negative (light bars) subpopulations. Data represent means ± S.E.M. of 2 independent experiments and were compared to the respective wild-type controls.

4.6. Misfolded proteins promote stress-induced cell death

Although misfolded proteins inhibited cell proliferation (Fig. 9B), we did not detect any necrosis by propidium iodide (PI) exclusion (data not shown). To investigate whether misfolded proteins would induce apoptosis, we performed analysis of total cellular DNA content by flow cytometry, where the sub-G1 peak is an indicator of late apoptotic cells. There was no increase in apoptosis in cells expressing GFP-degron or GFP-Δ9CAT, respectively (data not shown). Thus, short-term expression of misfolded proteins *per se* did not induce a significant cell loss. However, treatment of transfected cells with MG-132 resulted in an altered histogram with a distorted sub-G1 peak containing cell debris along with a marked decrease in the number of intact cells (Fig. 10A). Therefore, as a more appropriate marker of the number of intact (live) cells, a joint measure of cell proliferation and death, we calculated the area below the G1-S-G2/M peaks of GFP-positive cells (labeled by a horizontal arrow in Fig. 10A). GFP-degron and GFP-Δ9CAT transfection combined with MG-132 treatment resulted in a lesser amount of intact GFP-positive cells compared to their wild-type controls already at 37ºC (Fig. 10B). Importantly, there was a further sharp decrease in the number of GFP-degron- and GFP-Δ9CAT-transfected intact cells when they were given a moderate heat shock (43°C, 30 min), which did not have an effect on GFP- and GFP-wtCAT-expressing cells.

To obtain an independent measure of cell death, we performed annexin staining, detecting cell death from early apoptosis through late necrosis. GFP-positive cells displayed enhanced annexin staining compared with GFP-negative population and MG-132 treatment (2 μM, 42 h) resulted in an increased annexin positivity from around 10% to 25%, consistent with a general proteotoxicity induced by proteasome inhibition (Fig. 10C, compare GFP and GFP-wtCAT in the absence and presence of MG-132). Similarly to the previous propidium iodide and sub-G1 data, in the absence of MG-132, there was no significant difference between annexin staining of GFP-degron- and GFP-Δ9CAT-transfected cells compared to that of their wild-type counterparts (Fig. 10C). However, MG-132 treatment of cells expressing GFP-degron, but not GFP-Δ9CAT, yielded a significantly higher annexin positivity compared to controls (Fig. 10C, GFP: 25% *vs.*

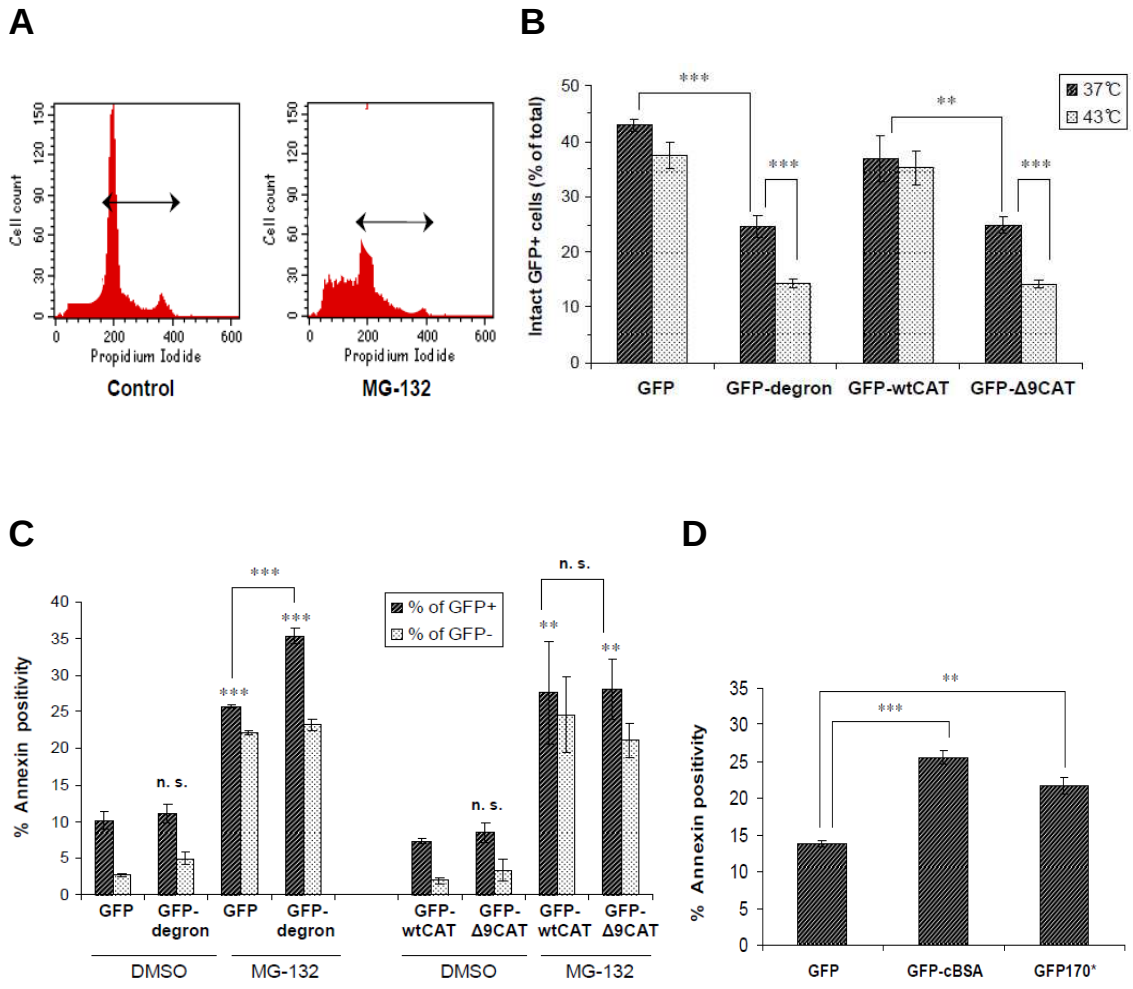

Figure 10. Misfolded proteins promote stress-induced cell death. (A) Cell cycle alterations observed during flow cytometric analyses of our protein models after treatment with MG-132. Combination of G1-S-G2/M peaks (representing intact cells) was chosen as the parameter for analysis of the following assay. **(B)** Misfolded proteins diminish survival of proteasome-inhibited cells upon a concomitant heat stress. Cells treated with MG-132 (2 μM, 20 h) were either incubated at 37°C (dark bars) or at 43°C for 30 min (light bars). The next day, cells were harvested and fixed overnight in ethanol at -20°C. After extraction of fragmented DNA, cells were stained with propidium iodide, and the remaining DNA content was analyzed by flow cytometry. Chart displays percentage of GFP-positive cells with an intact cell cycle out of the total cell population. Data represent means ± S.E.M. of 3 independent experiments and were compared with the respective wild-type controls for 37°C data and with their own 37°C controls for 43°C data. **(C)** Misfolded GFP-degron, but not GFP-Δ9CAT, induces annexin positivity upon proteasome inhibition. Cells treated with or without MG-132 (2 μM, 42 h) were stained with annexin V, and analyzed by flow cytometry. The chart shows the percentage of annexin positivity in GFP-positive (dark bars) and GFP-negative (light bars) subpopulations for each protein model. Data represent means ± S.E.M. of 3 independent experiments, and GFP-positive values were compared to GFP and GFP-wtCAT controls (asterisks on columns) and GFP-degron/GFP-Δ9CAT to their respective MG-132-treated wild-type control (linked bars). **(D)** GFP-cBSA and GFP170* induce cell death upon proteasome inhibition. Cells transfected with the indicated constructs were treated with MG-132 (2 μM, 42 h), after trypsinization were stained with annexin V, and analyzed by flow cytometry. The chart shows the percentage of annexin positivity in cells with GFP expression above 5×10^2 fluorescence intensity. Data represent means ± S.E.M. of 3 independent experiments and were compared to GFP.

GFP-degron: 35%). These results confirm the GFP-degron-related findings presented in Fig. 10B, and suggest that some form of GFP-Δ9CAT-induced cell death may escape detection by annexin in our experimental conditions. Nevertheless, when MG-132-treated GFP-Δ9CAT cells underwent a moderate heat shock (43°C, 30 min), they also displayed an increased annexin positivity comparable to that of GFP-degron (GFP-wtCAT: 27% *vs.* GFP-Δ9CAT: 37%). Moreover, we obtained similar results with two other non-native misfolded protein models, GFP-cBSA and GFP170* upon MG-132 treatment (Fig. 10D). Thus, diverse misfolded proteins sensitize cells to manifest enhanced cytotoxicity in response to stress.

4.7. HSF1, Hsp70 and SIRT1 protect from GFP-degron-induced cytotoxicity

We next addressed how genetic activation of stress-responsive mechanisms would combat the cytotoxicity induced by GFP-degron. HSF1 and Hsp70 are important determinants of the heat shock response, ameliorating toxicity of neurodegenerative models (see Section 1.4.1). SIRT1 is an NAD^+-dependent protein deacetylase, which was reported to control HSF1 activity by prolonging its DNA binding through deacetylation [227], and was recently shown to be required for the induction of Hsp70 expression upon heat shock in mouse embryonic fibroblasts [228]. It was also shown to be protective in initial studies against polyglutamine-induced cytotoxicity in both *C. elegans* and mammalian neurons [229], though its general role in invertebrate longevity has recently been questioned [230]. SIRT6 is a nuclear sirtuin paralog implicated in dietary restriction and the metabolic syndrome, however, there are no data on its role in proteostasis [231].

All the HSF1, Hsp70, SIRT1 and SIRT6 constructs were strongly overexpressed upon transfection (Fig. 11A). None of the constructs caused any significant difference in the number of GFP-degron-positive cells (i.e. cells expressing and not degrading GFP-degron) in the absence or presence of MG-132 (data not shown), suggesting they did not alter the turnover of GFP-degron. HSF1, Hsp70 and SIRT1 constructs were all found to

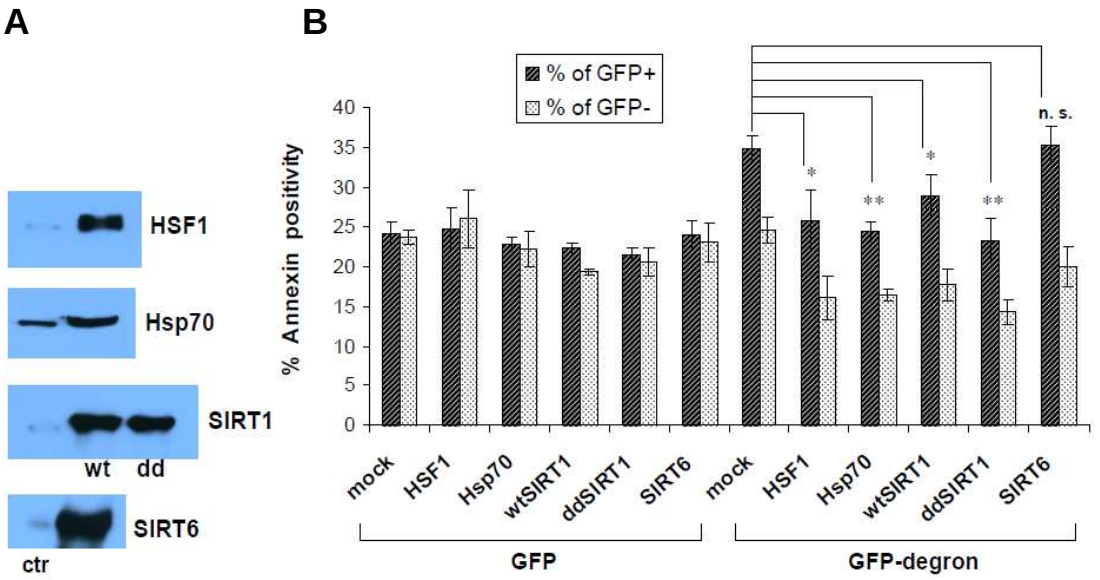

Figure 11. HSF1, Hsp70 and SIRT1 protect from GFP-degron-induced cytotoxicity. (A) HSF1, Hsp70, SIRT1s and SIRT6 are strongly overexpressed upon transfection. Cells were transfected with mock (ctr), HSF1, Hsp70, wtSIRT1, deacetylase-deficient H363Y mutant SIRT1 (ddSIRT1) and SIRT6 constructs for 24 h, lysed and analyzed by Western blotting for the respective proteins. Images are representatives of 2 independent experiments. **(B)** Cell death of MG-132-treated (2 μM, 42 h) cells. Cotransfections of the constructs were done at a ratio of 1:1 (misfolded protein construct: modulator). Annexin assay was performed as described in Materials and Methods. Chart shows the percentage of annexin positivity in GFP-positive (dark bars) and GFP-negative (light bars) subpopulations for each cotransfection. Renilla luciferase plasmid served as mock. Data represent means ± S.E.M. of 3 independent experiments. Statistical comparisons were made between the respective GFP+ samples compared to mock-cotransfected sample.

prevent cell death in MG-132-treated (2 μM, 42 h) GFP-degron-expressing cells, decreasing annexin positivity from 35% back to cca. 25% (Fig. 11B, cf. Fig. 10C). Interestingly, SIRT1-mediated recovery from GFP-degron-induced cytotoxicity was independent of the deacetylase activity of SIRT1, as both wildtype (wtSIRT1) and the deacetylase-deficient H363Y mutant (ddSIRT1) were protective. In contrast, SIRT6 did not exert a protective effect, giving an independent evidence for the specific action of SIRT1. This finding is in line with a recent study where SIRT1-induced neuroprotection was found to be independent of its deacetylase activity [232], suggesting a novel, non-catalytic mechanism of cytoprotection for SIRT1.

5. Discussion

Protein conformational diseases share common features: the accumulation of non-native protein species and a consequent cytotoxicity. In this study, we have isolated the general effects elicited by single misfolded polypeptides by expressing two *bona fide* inert misfolded proteins not occurring in the mammalian cytosol. Both GFP-fused degron and C-terminally truncated chloramphenicol acetyltransferase lost solubility and exhibited aggregation, transiently associated with and induced the expression of the chaperone Hsp70, underwent proteasome-dependent degradation in the majority of cells, induced growth arrest, and caused cytotoxicity in response to stress, which was ameliorated by stress-responsive mechanisms (Fig. 12). These features obtained with diverse misfolded proteins are consistent with an inherent toxicity of the misfolded ensembles *per se*.

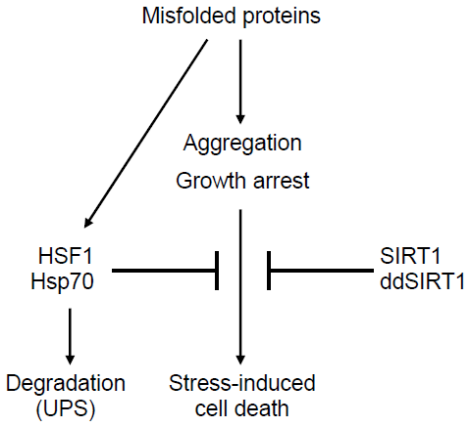

Figure 12. **Misfolded proteins in mammalian cells.** Misfolded proteins induce the heat shock response and are turned over by the UPS in the majority of cells. In cells that are incompetent to degrade them, they form aggregates and cause growth arrest. Upon various stresses, such as the inhibition of the UPS or heat shock, misfolded proteins promote cell death. The genetic upregulation of the heat shock response (HSF1 or Hsp70) and the sirtuin SIRT1, independently of its deacetylase activity (ddSIRT1), protects from stress-induced cytotoxicity.

The C-terminally truncated form of chloramphenicol acetyltransferase, Δ9CAT, has been previously shown to become unstable, lose chloramphenicol resistance, and form inclusion bodies in *Escherichia coli* [214-215]. Our results indicate GFP-Δ9CAT instability also induces its misfolding in mammalian cells (Figs. 5 and 6). The 16-residue

degron peptide supplements proteins with a C-terminal amphipathic α-helix conferring destabilization and proteasome-dependent degradation on the extended proteins such as yeast Ura3p [233-234] and GFP [61]. Therefore, GFP-degron appears to be a Janus-faced molecule, i.e. both an *in vivo* UPS reporter [61, 63, 235] and a misfolded protein (ref. [213] and present study, Fig. 5). This dual behavior can be explained by considering a primary misfolding of GFP-degron and its chaperone-mediated disposal by the ubiquitin-proteasome system (UPS) (ref. [213] and present study, Fig. 12), a pathway identical to that of global protein (mis)folding [79]. This model is supported by the similar phenotype (exhibiting decreased solubility, aggregation, chaperone induction, growth inhibition) of GFP-degron to several misfolded proteins: YFP point mutants in yeast [222], GFP170* (ref. [60] and present study) and GFP-Δ9CAT (present study), respectively. Besides, yeast Ura3p fused to degron requires the Hsp70/Hsp40 orthologs Ssa1p/Ydj1p for both its proteasomal degradation and solubility [236], in agreement with a degron-induced misfolding of Ura3p.

Our findings suggest that aggregate formation prevails, if the level of misfolded proteins exceeds the proteostatic capacity of the cell. Indeed, GFP-degron was efficiently cleared from all cells upon low level stable expression where proteasome capacity possessed an 80% reserve [61]. However, upon transient transfection in our study and in that of Link *et al.* [213], although misfolded proteins were still cleared from the majority of cell population (Fig. 6), they formed aggregates in GFP-positive cells (ref. [213] and Fig. 5B), which was augmented by proteasome inhibition (Fig. 6). Overexpression of Hsp70 or HSF1 did not decrease the number of GFP-degron-positive cells (i.e. did not increase the turnover of the protein), which along with the yeast study on Ura3p-degron [236] suggest that chaperones are required for but do not limit GFP-degron degradation. These findings suggest the UPS is a rate-limiting step in the chaperone-mediated disposal of misfolded proteins and offer a rationale for GFP-degron as an *in vivo* marker measuring UPS capacity.

The roles of Hsp70 and HSF1 in cells expressing misfolded proteins (Fig. 11) corroborate the well-documented role of the heat shock response in the recognition and defense

against proteotoxicity (see Section 1.4.1). The decreasing order of intensity of Hsp70 induction by GFP-degron > GFP-Δ9CAT > GFP-cBSA=GFP170* indicates a proportional release of HSF1 from its repressing chaperone-complex in response to misfolding. This effect is consistent with the previously reported, dose-dependent effect of cytosolic BSA on HSF1 activation [220]. Considering the ~1-2% maximal level of misfolded proteins induced by proteasome inhibition (Fig. 6) and an induction of Hsp70 in the heat-shock range (Fig. 7), we speculate that misfolded ensembles above the 0.02% to 0.04% threshold level may elicit a signal potent enough to provoke a significant threat, namely cell cycle arrest (Fig. 9). This threat, however, appears to be compensated in our experimental conditions by a highly efficient recognition/disposal, as demonstrated by the negligible effects of misfolded protein expression on thermotolerance and on cytotoxicity (Fig. 10C, DMSO bars). Recent studies demonstrate a specific, HSF1-mediated cytosolic unfolded protein response within the wider heat shock response/proteostatic network in yeast and plants [221-222, 237-238]. Our results by showing a selective activation of *hsp70* vs. the ER stress marker *grp78* promoter (Fig. 7A and data not shown) extend the existence of this specific cytosolic response to mammalian cells. The misfolded proteins used in this study provide a tractable model to identify the cytosolic unfolded protein response at the systems level in mammalian cells.

We observed a differential, but modest effect of GFP-degron and GFP-Δ9CAT on firefly luciferase folding (Fig. 8). The reason for this difference is unknown. It may be that GFP-degron and GFP-Δ9CAT differentially affect protein transcription/translation. Though we did not test luciferase mRNA and protein levels, the similar β-galactosidase activities and the equal residual activities after heat shock or MG-132 treatment exclude such a possibility. The GFP-Δ9CAT-induced luciferase activation may be explained by its less pronounced effects (i.e. higher ratio of GFP-positive cells, slower turnover, smaller *hsp70* promoter induction and decreased inhibition of cell proliferation), suggesting less toxic misfolded species formed by GFP-Δ9CAT, which in turn may activate chaperone-mediated folding. Though these data do not allow a clear conclusion, the modest effects and the clear dissection from toxicity (Figs. 9 and 10) suggest chaperone-mediated folding is not the major determinant of short-term action of individual misfolded proteins.

Our results in COS-7 cells recapitulate the proliferation arrest obtained with single misfolded mutants including polyQ103-GFP in HEK-293 cells [61], mutant SOD1 in neuroblastoma N2a cells [239], GFP170* in COS-7 cells [60], YFP mutants [222] and the proline analog azetidine-carboxylate in yeast [240], which suggests a conserved, general effect of protein misfolding. This occurs in GFP-positive cells (i.e. cells that are unable to degrade the misfolded proteins, Fig. 12). The almost, but not entirely complete loss of BrdU incorporation with misfolded proteins may be consistent with both G1 and G2/M arrest (Fig. 9B). As in COS-7 cells the SV40 large T-antigen inactivates both Rb and p53, it is tempting to speculate that mechanisms distinct from these checkpoint responses may inhibit proliferation. Indeed, such mechanisms arising from the inherent toxicity of misfolding have been demonstrated, such as destabilization and/or sequestration into aggregates of the growth-promoting transcription factors CBP and TBP [52-53, 60] (see Section 1.3). More evidence supporting this possibility has come from a recent study where amyloid-like aggregates of non-native, artificial β-sheet proteins were shown to sequester an extensive list of metastable proteins with key roles in chromatin organization, transcription, translation, maintenance of cell architecture and protein quality control [241]. Alternatively, growth inhibition may be due to the adaptive response, e.g. HSF1 mediating reversible cell cycle arrest in yeast [240] or increased Hsp70 inhibiting growth [242-243]. Though the underlying molecular pathways remain to be analyzed, our findings on decreased replicative capacity of transformed cells induced by misfolded proteins might have a potential impact in non-transformed mitotic cells or stem cells.

A number of studies demonstrated extensive apoptosis using disease-associated mutants including huntingtin [35, 146], amyloid-β [244], α-synuclein [245] and SOD1 [246] in cell (mostly neuronal) culture and animal models. However, we have not been able to detect death of immortalized COS-7 cells expressing misfolded proteins in non-stress conditions during the time-scale of our experiments. Whether the long-term expression of a single misfolded protein leads to cell loss requires further studies. We also consider the possibility that misfolded proteins may induce cytotoxicity in neurons, where proteostatic

defenses, such as the heat shock response are inherently weaker [104, 247]. Moreover, paralysis in the absence of apoptosis in *C. elegans* muscle expressing GFP-degron [213] and proliferation arrest (our study) suggest that severe dysfunctionality does not necessarily need cell death. The augmentation of death observed upon proteasome inhibition or heat shock by 4 misfolded mutants (Fig. 10) indicates that already a short-term expression of misfolded ensembles compromise cells to mount an efficient adaptive response to proteotoxic stress. Defective stress tolerance seems to be a deleterious consequence of misfolding, as upregulation of two stress-responsive mechanisms, the heat shock response (HSF1 and Hsp70) as well as the sirtuin SIRT1, conferred protection (Fig. 11). Our findings extend earlier studies on the beneficial role of chaperones in various cell culture and animal models of protein misfolding (see Section 1.4.1 and ref. [213]). The cytoprotective effect by chaperones may either lie in the restoration of protein homeostasis and/or the negative regulation by Hsp70 of death signals via p38 and JNK [143-145].

Our findings on the SIRT1 overexpression protecting from GFP-degron-induced proteotoxicity confirm previous results involving neurodegenerative models of polyglutamine [229, 248], amyloid-β [249], α-synuclein [228, 249] and SOD1 [250]. Moreover, the lack of effect of SIRT6 overexpression indicates divergent roles for sirtuin paralogs in mammals. SIRT1-dependent deacetylation of key signaling molecules including HSF1 [227-228] and consequent cellular events have been extensively reported [251-252]. However, our study did not demonstrate a requirement of deacetylase activity, suggesting the SIRT1-mediated cytoprotective response did not demand an increased deacetylation/activation of HSF1 in our model (Fig. 11B). Recently, growing body of evidence shows deacetylase-independent functions of SIRT1 [253-255] including neuroprotection [232], however, the molecular mechanism of SIRT1 remains enigmatic. Our results extend these functions to protein misfolding, and recall tests on the involvement of SIRT1 deacetylase activity in protection from neurodegenerative disease models [228-229, 248-250]. Finding the proper role for SIRT1 is especially important in the light of a recent study demonstrating the inability of SIRT1 orthologs to extend

lifespan in invertebrates [230], which has implications for the development and use of SIRT1 activators as potential drug candidates [256].

Our results show that the action of misfolded proteins depends on the proteostatic balance and cellular heterogeneity. Protein misfolding is not limited to single genes/proteins, but it rather involves a significant fraction of the proteome probably due to destabilizing SNPs [113], mistranslation [3, 224, 257], and post-translational modifications: we note that the level of misfolded proteins in our study is comparable to protein carbonyls in aged tissues [4-5, 8]. Lack of dilution of damage as well as the age-associated collapse and/or intrinsic weakness of proteostasis precipitate symptoms particularly in postmitotic neurons during aging [104, 187, 247]. Our findings raise a question whether protein misfolding would induce damage to the replicative compartment *in situ* which may have implications in aging of regenerating tissues. Indeed, dystrophy of hair follicles has been reported in a mistranslation mouse model [3]. Detrimental outcome of misfolding may also shape the evolution of tumors, where intensive growth (translation) and high stress are associated with the absolute reliance on HSF1 [258]. These hypotheses, as well as the long-term effects of misfolded proteins on cellular fitness are subjects of future studies.

6. Conclusion

In this study, we have investigated the impact of protein misfolding *per se* in transformed mammalian cells by characterizing two unrelated destabilized proteins, devoid of disease-associated repeat expansions, specific cellular functions and interaction partners. Using GFP and GFP-wtCAT as controls, we demonstrate that both GFP-degron and GFP-Δ9CAT display characteristics of protein misfolding. We find that transient expression of these misfolded proteins does not induce cell death. However, they do induce cell proliferation arrest in cells that are unable to degrade them, suggesting a potential inhibitory effect of protein misfolding on cell growth in replicating mitotic cells. We further show that upon various stress conditions such as proteasome inhibition by MG-132 or heat shock, misfolded proteins augment cell death, suggesting that cells have a limited proteostatic capacity and a compromise of this capacity potentiates the cytotoxicity of misfolded ensembles, which concomitantly sensitize cells to manifest increased susceptibility to proteotoxic stress. Finally, we provide evidence that genetic upregulation of two stress-responsive mechanisms, the heat shock response (HSF1 and Hsp70) and the sirtuin SIRT1, confers protection against stress-induced cell death. Notably, the deacetylase-deficient mutant (H363Y) form of SIRT1 proves to be equally protective, extending the recently reported non-catalytic beneficial effects of SIRT1 to protein misfolding. As a conclusion, our study provides a mammalian cellular model of misfolded proteins and reveals that short-term expression of single misfolded proteins independently of sequence and function inhibits proliferation and stress adaptation in replicating cells that can be prevented by upregulation of stress-responsive mechanisms.

7. Abstract

Protein misfolding is implicated in neurodegenerative diseases and occurs in aging. However, the contribution of the misfolded ensembles *per se* to toxicity remains largely unknown. During my Ph.D. studies, I have introduced two primate cell models of destabilized proteins devoid of all repeat expansions, specific cellular functions and interactors, as *bona fide* misfolded proteins, allowing us to isolate the gain-of-function of non-native structures. Both GFP-degron and a mutant chloramphenicol acetyltransferase fused to GFP (GFP-Δ9CAT), similarly to well-known disease-associated mutant proteins, exhibit decreased solubility, form perinuclear aggregates, activate the heat shock response, colocalize with and induce the chaperone Hsp70 (HSPA1A/B), and are degraded by the proteasome in COS-7 SV40-transformed monkey kidney fibroblast-like cells. We find that transient expression of misfolded proteins neither significantly compromise chaperone-mediated folding capacity nor induce cell death. However, they do induce growth arrest in cells that are unable to degrade them and promote stress-induced cell death upon proteasome inhibition by MG-132 and heat shock. Finally, we show that overexpression of heat shock transcription factor HSF1 and Hsp70, as well as wildtype and deacetylase-deficient (H363Y) SIRT1 sirtuin restores survival upon stress, implying a non-catalytic action of SIRT1 in response to protein misfolding. Our study establishes a novel model of protein misfolding and extends our knowledge on the mechanism of the function-independent proteotoxicity of misfolded proteins in dividing cells, which may contribute to conformational diseases and aging.

8. Összefoglalás

A fehérje denaturáció kóroki szerepet játszik számos neurodegeneratív betegségben és fokozódik az öregedés során. Azonban a denaturált fehérje szerkezet szekvenciától függetlenül kifejtett általános hatása a sejt funkcióra és toxicitásra jórészt ismeretlen. Ph.D. munkám során létrehoztam és jellemeztem két sejtes destabilizált kitekert fehérje modellt, melyek nem tartalmaznak aggregáció-indukáló repetitív szekvenciákat, továbbá nincs specifikus funkciójuk, sem interakciós partnereik az emlős sejtekben. Ezek a tulajdonságok lehetővé tették, hogy a szelektíven a nem-natív fehérjeszerkezet általános funkciónyerő hatását tanulmányozzam. Eredményeim szerint a GFP-degron és a GFP-vel fúzionált mutáns kloramfenikol-acetiltranszferáz (GFP-Δ9CAT) fehérjék a jól ismert konformációs betegségokozó mutánsokhoz hasonlóan csökkent szolubilitásúak, perinukleáris aggregátumokat képeznek, lebontásukért a proteaszóma felelős, valamint kolokalizációt mutatnak és transzkripcionálisan indukálják a Hsp70 (HSPA1A/B) chaperon fehérjéket COS-7 SV40-transzformált majomvese fibroblaszt sejtekben. A GFP-degron és a GFP-Δ9CAT átmeneti expressziója nem gátolja jelentősen a chaperon-függő fehérjetekerő kapacitást és nem okoz sejthalált, azonban sejtciklus leállást okoz azokban a sejtekben, melyek nem képesek lebontani a kitekert konformereket. Ezen felül elősegítik a hősokkal és proteaszóma gátló MG-132 kezeléssel kiváltott proteotoxikus stresszre bekövetkező sejthalált. A hősokk transzkripciós factor HSF1 és a Hsp70, valamint a vad típusú és deacetiláz-deficiens (H363Y) SIRT1 szirtuin túltermelése egyaránt megelőzi a stressz-indukálta sejthalált, ami a stresszválaszok védő hatásán túl a SIRT1 új, nem-katalitikus funkciójára enged következtetni. Összefoglalva, a doktori munkám során létrehozott nemspecifikus kitekert fehérje modell feltárja a fehérje denaturáció funkciótól független, osztódó sejtekben is megfigyelhető proteotoxikus hatását, mely hozzájárulhat a konformációs betegségek kifejlődéséhez és az öregedéshez.

9. References

1. Soto C. (2003) Unfolding the role of protein misfolding in neurodegenerative diseases. *Nat Rev Neurosci* **4**(1), 49-60
2. Carrell R. W., and Lomas D. A. (1997) Conformational disease. *Lancet* **350**(9071), 134-138
3. Lee J. W., Beebe K., Nangle L. A., Jang J., Longo-Guess C. M., Cook S. A., Davisson M. T., Sundberg J. P., Schimmel P., and Ackerman S. L. (2006) Editing-defective tRNA synthetase causes protein misfolding and neurodegeneration. *Nature* **443**(7107), 50-55
4. Squier T. C. (2001) Oxidative stress and protein aggregation during biological aging. *Exp Gerontol* **36**(9), 1539-1550
5. Stadtman E. R., and Levine R. L. (2003) Free radical-mediated oxidation of free amino acids and amino acid residues in proteins. *Amino Acids* **25**(3-4), 207-218
6. Ross C. A., and Poirier M. A. (2004) Protein aggregation and neurodegenerative disease. *Nat Med* **10 Suppl,** S10-17
7. Morimoto R. I. (2008) Proteotoxic stress and inducible chaperone networks in neurodegenerative disease and aging. *Genes Dev* **22**(11), 1427-1438
8. Dobson C. M. (2003) Protein folding and misfolding. *Nature* **426**(6968), 884-890
9. Johnston J. A., Ward C. L., and Kopito R. R. (1998) Aggresomes: a cellular response to misfolded proteins. *J Cell Biol* **143**(7), 1883-1898
10. Stefani M. (2004) Protein misfolding and aggregation: new examples in medicine and biology of the dark side of the protein world. *Biochim Biophys Acta* **1739**(1), 5-25
11. Ross C. A., and Poirier M. A. (2005) Opinion: What is the role of protein aggregation in neurodegeneration? *Nat Rev Mol Cell Biol* **6**(11), 891-898
12. Taylor J. P., Hardy J., and Fischbeck K. H. (2002) Toxic proteins in neurodegenerative disease. *Science* **296**(5575), 1991-1995
13. Sunde M., Serpell L. C., Bartlam M., Fraser P. E., Pepys M. B., and Blake C. C. (1997) Common core structure of amyloid fibrils by synchrotron X-ray diffraction. *J Mol Biol* **273**(3), 729-739

14. Petkova A. T., Ishii Y., Balbach J. J., Antzutkin O. N., Leapman R. D., Delaglio F., and Tycko R. (2002) A structural model for Alzheimer's beta-amyloid fibrils based on experimental constraints from solid state NMR. *Proc Natl Acad Sci U S A* **99**(26), 16742-16747
15. Serpell L. C., Blake C. C., and Fraser P. E. (2000) Molecular structure of a fibrillar Alzheimer's A beta fragment. *Biochemistry* **39**(43), 13269-13275
16. Serpell L. C., Berriman J., Jakes R., Goedert M., and Crowther R. A. (2000) Fiber diffraction of synthetic alpha-synuclein filaments shows amyloid-like cross-beta conformation. *Proc Natl Acad Sci U S A* **97**(9), 4897-4902
17. Scherzinger E., Lurz R., Turmaine M., Mangiarini L., Hollenbach B., Hasenbank R., Bates G. P., Davies S. W., Lehrach H., and Wanker E. E. (1997) Huntingtin-encoded polyglutamine expansions form amyloid-like protein aggregates in vitro and in vivo. *Cell* **90**(3), 549-558
18. Chattopadhyay M., and Valentine J. S. (2009) Aggregation of copper-zinc superoxide dismutase in familial and sporadic ALS. *Antioxid Redox Signal* **11**(7), 1603-1614
19. Sadqi M., Hernandez F., Pan U., Perez M., Schaeberle M. D., Avila J., and Munoz V. (2002) Alpha-helix structure in Alzheimer's disease aggregates of tau-protein. *Biochemistry* **41**(22), 7150-7155
20. Chiti F., Webster P., Taddei N., Clark A., Stefani M., Ramponi G., and Dobson C. M. (1999) Designing conditions for in vitro formation of amyloid protofilaments and fibrils. *Proc Natl Acad Sci U S A* **96**(7), 3590-3594
21. Fandrich M., Fletcher M. A., and Dobson C. M. (2001) Amyloid fibrils from muscle myoglobin. *Nature* **410**(6825), 165-166
22. Chiti F., Stefani M., Taddei N., Ramponi G., and Dobson C. M. (2003) Rationalization of the effects of mutations on peptide and protein aggregation rates. *Nature* **424**(6950), 805-808
23. Petkova A. T., Leapman R. D., Guo Z., Yau W. M., Mattson M. P., and Tycko R. (2005) Self-propagating, molecular-level polymorphism in Alzheimer's beta-amyloid fibrils. *Science* **307**(5707), 262-265

24. Bitan G., Kirkitadze M. D., Lomakin A., Vollers S. S., Benedek G. B., and Teplow D. B. (2003) Amyloid beta -protein (Abeta) assembly: Abeta 40 and Abeta 42 oligomerize through distinct pathways. *Proc Natl Acad Sci U S A* **100**(1), 330-335
25. Scherzinger E., Sittler A., Schweiger K., Heiser V., Lurz R., Hasenbank R., Bates G. P., Lehrach H., and Wanker E. E. (1999) Self-assembly of polyglutamine-containing huntingtin fragments into amyloid-like fibrils: implications for Huntington's disease pathology. *Proc Natl Acad Sci U S A* **96**(8), 4604-4609
26. Chen S., Berthelier V., Hamilton J. B., O'Nuallain B., and Wetzel R. (2002) Amyloid-like features of polyglutamine aggregates and their assembly kinetics. *Biochemistry* **41**(23), 7391-7399
27. Walsh D. M., Lomakin A., Benedek G. B., Condron M. M., and Teplow D. B. (1997) Amyloid beta-protein fibrillogenesis. Detection of a protofibrillar intermediate. *J Biol Chem* **272**(35), 22364-22372
28. Walsh D. M., Hartley D. M., Kusumoto Y., Fezoui Y., Condron M. M., Lomakin A., Benedek G. B., Selkoe D. J., and Teplow D. B. (1999) Amyloid beta-protein fibrillogenesis. Structure and biological activity of protofibrillar intermediates. *J Biol Chem* **274**(36), 25945-25952
29. Harper J. D., Wong S. S., Lieber C. M., and Lansbury P. T., Jr. (1999) Assembly of A beta amyloid protofibrils: an in vitro model for a possible early event in Alzheimer's disease. *Biochemistry* **38**(28), 8972-8980
30. Kopito R. R. (2000) Aggresomes, inclusion bodies and protein aggregation. *Trends Cell Biol* **10**(12), 524-530
31. Khurana R., Ionescu-Zanetti C., Pope M., Li J., Nielson L., Ramirez-Alvarado M., Regan L., Fink A. L., and Carter S. A. (2003) A general model for amyloid fibril assembly based on morphological studies using atomic force microscopy. *Biophys J* **85**(2), 1135-1144
32. Mattson M. P. (2000) Apoptosis in neurodegenerative disorders. *Nat Rev Mol Cell Biol* **1**(2), 120-129
33. Gutekunst C. A., Li S. H., Yi H., Mulroy J. S., Kuemmerle S., Jones R., Rye D., Ferrante R. J., Hersch S. M., and Li X. J. (1999) Nuclear and neuropil aggregates

in Huntington's disease: relationship to neuropathology. *J Neurosci* **19**(7), 2522-2534

34. Kuemmerle S., Gutekunst C. A., Klein A. M., Li X. J., Li S. H., Beal M. F., Hersch S. M., and Ferrante R. J. (1999) Huntington aggregates may not predict neuronal death in Huntington's disease. *Ann Neurol* **46**(6), 842-849
35. Saudou F., Finkbeiner S., Devys D., and Greenberg M. E. (1998) Huntingtin acts in the nucleus to induce apoptosis but death does not correlate with the formation of intranuclear inclusions. *Cell* **95**(1), 55-66
36. Katzman R., Terry R., DeTeresa R., Brown T., Davies P., Fuld P., Renbing X., and Peck A. (1988) Clinical, pathological, and neurochemical changes in dementia: a subgroup with preserved mental status and numerous neocortical plaques. *Ann Neurol* **23**(2), 138-144
37. Tompkins M. M., and Hill W. D. (1997) Contribution of somal Lewy bodies to neuronal death. *Brain Res* **775**(1-2), 24-29
38. Klement I. A., Skinner P. J., Kaytor M. D., Yi H., Hersch S. M., Clark H. B., Zoghbi H. Y., and Orr H. T. (1998) Ataxin-1 nuclear localization and aggregation: role in polyglutamine-induced disease in SCA1 transgenic mice. *Cell* **95**(1), 41-53
39. Lambert M. P., Barlow A. K., Chromy B. A., Edwards C., Freed R., Liosatos M., Morgan T. E., Rozovsky I., Trommer B., Viola K. L., Wals P., Zhang C., Finch C. E., Krafft G. A., and Klein W. L. (1998) Diffusible, nonfibrillar ligands derived from Abeta1-42 are potent central nervous system neurotoxins. *Proc Natl Acad Sci U S A* **95**(11), 6448-6453
40. Hartley D. M., Walsh D. M., Ye C. P., Diehl T., Vasquez S., Vassilev P. M., Teplow D. B., and Selkoe D. J. (1999) Protofibrillar intermediates of amyloid beta-protein induce acute electrophysiological changes and progressive neurotoxicity in cortical neurons. *J Neurosci* **19**(20), 8876-8884
41. Walsh D. M., Klyubin I., Fadeeva J. V., Cullen W. K., Anwyl R., Wolfe M. S., Rowan M. J., and Selkoe D. J. (2002) Naturally secreted oligomers of amyloid beta protein potently inhibit hippocampal long-term potentiation in vivo. *Nature* **416**(6880), 535-539

42. Gong Y., Chang L., Viola K. L., Lacor P. N., Lambert M. P., Finch C. E., Krafft G. A., and Klein W. L. (2003) Alzheimer's disease-affected brain: presence of oligomeric A beta ligands (ADDLs) suggests a molecular basis for reversible memory loss. *Proc Natl Acad Sci U S A* **100**(18), 10417-10422
43. Klyubin I., Walsh D. M., Lemere C. A., Cullen W. K., Shankar G. M., Betts V., Spooner E. T., Jiang L., Anwyl R., Selkoe D. J., and Rowan M. J. (2005) Amyloid beta protein immunotherapy neutralizes Abeta oligomers that disrupt synaptic plasticity in vivo. *Nat Med* **11**(5), 556-561
44. Sanchez I., Mahlke C., and Yuan J. (2003) Pivotal role of oligomerization in expanded polyglutamine neurodegenerative disorders. *Nature* **421**(6921), 373-379
45. Watase K., Weeber E. J., Xu B., Antalffy B., Yuva-Paylor L., Hashimoto K., Kano M., Atkinson R., Sun Y., Armstrong D. L., Sweatt J. D., Orr H. T., Paylor R., and Zoghbi H. Y. (2002) A long CAG repeat in the mouse Sca1 locus replicates SCA1 features and reveals the impact of protein solubility on selective neurodegeneration. *Neuron* **34**(6), 905-919
46. Arrasate M., Mitra S., Schweitzer E. S., Segal M. R., and Finkbeiner S. (2004) Inclusion body formation reduces levels of mutant huntingtin and the risk of neuronal death. *Nature* **431**(7010), 805-810
47. Tanaka M., Kim Y. M., Lee G., Junn E., Iwatsubo T., and Mouradian M. M. (2004) Aggresomes formed by alpha-synuclein and synphilin-1 are cytoprotective. *J Biol Chem* **279**(6), 4625-4631
48. Mukai H., Isagawa T., Goyama E., Tanaka S., Bence N. F., Tamura A., Ono Y., and Kopito R. R. (2005) Formation of morphologically similar globular aggregates from diverse aggregation-prone proteins in mammalian cells. *Proc Natl Acad Sci U S A* **102**(31), 10887-10892
49. Poirier M. A., Li H., Macosko J., Cai S., Amzel M., and Ross C. A. (2002) Huntingtin spheroids and protofibrils as precursors in polyglutamine fibrilization. *J Biol Chem* **277**(43), 41032-41037
50. Kayed R., Head E., Thompson J. L., McIntire T. M., Milton S. C., Cotman C. W., and Glabe C. G. (2003) Common structure of soluble amyloid oligomers implies common mechanism of pathogenesis. *Science* **300**(5618), 486-489

51. Bucciantini M., Giannoni E., Chiti F., Baroni F., Formigli L., Zurdo J., Taddei N., Ramponi G., Dobson C. M., and Stefani M. (2002) Inherent toxicity of aggregates implies a common mechanism for protein misfolding diseases. *Nature* **416**(6880), 507-511

52. Nucifora F. C., Jr., Sasaki M., Peters M. F., Huang H., Cooper J. K., Yamada M., Takahashi H., Tsuji S., Troncoso J., Dawson V. L., Dawson T. M., and Ross C. A. (2001) Interference by huntingtin and atrophin-1 with cbp-mediated transcription leading to cellular toxicity. *Science* **291**(5512), 2423-2428

53. Schaffar G., Breuer P., Boteva R., Behrends C., Tzvetkov N., Strippel N., Sakahira H., Siegers K., Hayer-Hartl M., and Hartl F. U. (2004) Cellular toxicity of polyglutamine expansion proteins: mechanism of transcription factor deactivation. *Mol Cell* **15**(1), 95-105

54. Suhr S. T., Senut M. C., Whitelegge J. P., Faull K. F., Cuizon D. B., and Gage F. H. (2001) Identities of sequestered proteins in aggregates from cells with induced polyglutamine expression. *J Cell Biol* **153**(2), 283-294

55. Steffan J. S., Kazantsev A., Spasic-Boskovic O., Greenwald M., Zhu Y. Z., Gohler H., Wanker E. E., Bates G. P., Housman D. E., and Thompson L. M. (2000) The Huntington's disease protein interacts with p53 and CREB-binding protein and represses transcription. *Proc Natl Acad Sci U S A* **97**(12), 6763-6768

56. Cummings C. J., Mancini M. A., Antalffy B., DeFranco D. B., Orr H. T., and Zoghbi H. Y. (1998) Chaperone suppression of aggregation and altered subcellular proteasome localization imply protein misfolding in SCA1. *Nat Genet* **19**(2), 148-154

57. Waelter S., Boeddrich A., Lurz R., Scherzinger E., Lueder G., Lehrach H., and Wanker E. E. (2001) Accumulation of mutant huntingtin fragments in aggresome-like inclusion bodies as a result of insufficient protein degradation. *Mol Biol Cell* **12**(5), 1393-1407

58. Davies S. W., Turmaine M., Cozens B. A., DiFiglia M., Sharp A. H., Ross C. A., Scherzinger E., Wanker E. E., Mangiarini L., and Bates G. P. (1997) Formation of neuronal intranuclear inclusions underlies the neurological dysfunction in mice transgenic for the HD mutation. *Cell* **90**(3), 537-548

59. Perry G., Friedman R., Shaw G., and Chau V. (1987) Ubiquitin is detected in neurofibrillary tangles and senile plaque neurites of Alzheimer disease brains. *Proc Natl Acad Sci U S A* **84**(9), 3033-3036
60. Fu L., Gao Y. S., and Sztul E. (2005) Transcriptional repression and cell death induced by nuclear aggregates of non-polyglutamine protein. *Neurobiol Dis* **20**(3), 656-665
61. Bence N. F., Sampat R. M., and Kopito R. R. (2001) Impairment of the ubiquitin-proteasome system by protein aggregation. *Science* **292**(5521), 1552-1555
62. Hershko A., and Ciechanover A. (1998) The ubiquitin system. *Annu Rev Biochem* **67**, 425-479
63. Bennett E. J., Bence N. F., Jayakumar R., and Kopito R. R. (2005) Global impairment of the ubiquitin-proteasome system by nuclear or cytoplasmic protein aggregates precedes inclusion body formation. *Mol Cell* **17**(3), 351-365
64. Sakahira H., Breuer P., Hayer-Hartl M. K., and Hartl F. U. (2002) Molecular chaperones as modulators of polyglutamine protein aggregation and toxicity. *Proc Natl Acad Sci U S A* **99**(Suppl 4), 16412-16418
65. Venkatraman P., Wetzel R., Tanaka M., Nukina N., and Goldberg A. L. (2004) Eukaryotic proteasomes cannot digest polyglutamine sequences and release them during degradation of polyglutamine-containing proteins. *Mol Cell* **14**(1), 95-104
66. Holmberg C. I., Staniszewski K. E., Mensah K. N., Matouschek A., and Morimoto R. I. (2004) Inefficient degradation of truncated polyglutamine proteins by the proteasome. *EMBO J* **23**(21), 4307-4318
67. Matsumoto G., Stojanovic A., Holmberg C. I., Kim S., and Morimoto R. I. (2005) Structural properties and neuronal toxicity of amyotrophic lateral sclerosis-associated Cu/Zn superoxide dismutase 1 aggregates. *J Cell Biol* **171**(1), 75-85
68. Dantuma N. P., Groothuis T. A., Salomons F. A., and Neefjes J. (2006) A dynamic ubiquitin equilibrium couples proteasomal activity to chromatin remodeling. *J Cell Biol* **173**(1), 19-26
69. Hicke L. (2001) Protein regulation by monoubiquitin. *Nat Rev Mol Cell Biol* **2**(3), 195-201

70. Cuervo A. M., Stefanis L., Fredenburg R., Lansbury P. T., and Sulzer D. (2004) Impaired degradation of mutant alpha-synuclein by chaperone-mediated autophagy. *Science* **305**(5688), 1292-1295
71. Massey A. C., Kaushik S., Sovak G., Kiffin R., and Cuervo A. M. (2006) Consequences of the selective blockage of chaperone-mediated autophagy. *Proc Natl Acad Sci U S A* **103**(15), 5805-5810
72. Lashuel H. A., Hartley D., Petre B. M., Walz T., and Lansbury P. T., Jr. (2002) Neurodegenerative disease: amyloid pores from pathogenic mutations. *Nature* **418**(6895), 291
73. Quist A., Doudevski I., Lin H., Azimova R., Ng D., Frangione B., Kagan B., Ghiso J., and Lal R. (2005) Amyloid ion channels: a common structural link for protein-misfolding disease. *Proc Natl Acad Sci U S A* **102**(30), 10427-10432
74. Lin H., Bhatia R., and Lal R. (2001) Amyloid beta protein forms ion channels: implications for Alzheimer's disease pathophysiology. *FASEB J* **15**(13), 2433-2444
75. Kawahara M., Kuroda Y., Arispe N., and Rojas E. (2000) Alzheimer's beta-amyloid, human islet amylin, and prion protein fragment evoke intracellular free calcium elevations by a common mechanism in a hypothalamic GnRH neuronal cell line. *J Biol Chem* **275**(19), 14077-14083
76. Orrenius S., Zhivotovsky B., and Nicotera P. (2003) Regulation of cell death: the calcium-apoptosis link. *Nat Rev Mol Cell Biol* **4**(7), 552-565
77. Bucciantini M., Calloni G., Chiti F., Formigli L., Nosi D., Dobson C. M., and Stefani M. (2004) Prefibrillar amyloid protein aggregates share common features of cytotoxicity. *J Biol Chem* **279**(30), 31374-31382
78. Sherman M. Y., and Goldberg A. L. (2001) Cellular defenses against unfolded proteins: a cell biologist thinks about neurodegenerative diseases. *Neuron* **29**(1), 15-32
79. Hartl F. U., and Hayer-Hartl M. (2002) Molecular chaperones in the cytosol: from nascent chain to folded protein. *Science* **295**(5561), 1852-1858
80. Tyedmers J., Mogk A., and Bukau B. (2010) Cellular strategies for controlling protein aggregation. *Nat Rev Mol Cell Biol* **11**(11), 777-788

81. Chiti F., and Dobson C. M. (2006) Protein misfolding, functional amyloid, and human disease. *Annu Rev Biochem* **75**, 333-366
82. Ellis R. J. (2001) Macromolecular crowding: obvious but underappreciated. *Trends Biochem Sci* **26**(10), 597-604
83. Powers E. T., Morimoto R. I., Dillin A., Kelly J. W., and Balch W. E. (2009) Biological and chemical approaches to diseases of proteostasis deficiency. *Annu Rev Biochem* **78**, 959-991
84. Buchberger A., Bukau B., and Sommer T. (2010) Protein quality control in the cytosol and the endoplasmic reticulum: brothers in arms. *Mol Cell* **40**(2), 238-252
85. Kampinga H. H., and Craig E. A. (2010) The HSP70 chaperone machinery: J proteins as drivers of functional specificity. *Nat Rev Mol Cell Biol* **11**(8), 579-592
86. Goldberg A. L. (2003) Protein degradation and protection against misfolded or damaged proteins. *Nature* **426**(6968), 895-899
87. Ballinger C. A., Connell P., Wu Y., Hu Z., Thompson L. J., Yin L. Y., and Patterson C. (1999) Identification of CHIP, a novel tetratricopeptide repeat-containing protein that interacts with heat shock proteins and negatively regulates chaperone functions. *Mol Cell Biol* **19**(6), 4535-4545
88. Murata S., Minami Y., Minami M., Chiba T., and Tanaka K. (2001) CHIP is a chaperone-dependent E3 ligase that ubiquitylates unfolded protein. *EMBO Rep* **2**(12), 1133-1138
89. Meacham G. C., Patterson C., Zhang W., Younger J. M., and Cyr D. M. (2001) The Hsc70 co-chaperone CHIP targets immature CFTR for proteasomal degradation. *Nat Cell Biol* **3**(1), 100-105
90. Luders J., Demand J., and Hohfeld J. (2000) The ubiquitin-related BAG-1 provides a link between the molecular chaperones Hsc70/Hsp70 and the proteasome. *J Biol Chem* **275**(7), 4613-4617
91. Demand J., Alberti S., Patterson C., and Hohfeld J. (2001) Cooperation of a ubiquitin domain protein and an E3 ubiquitin ligase during chaperone/proteasome coupling. *Curr Biol* **11**(20), 1569-1577
92. Zhang X., and Qian S. B. (2011) Chaperone-mediated hierarchical control in targeting misfolded proteins to aggresomes. *Mol Biol Cell* **22**(18), 3277-3288

93. Gamerdinger M., Kaya A. M., Wolfrum U., Clement A. M., and Behl C. (2011) BAG3 mediates chaperone-based aggresome-targeting and selective autophagy of misfolded proteins. *EMBO Rep* **12**(2), 149-156
94. Massey A., Kiffin R., and Cuervo A. M. (2004) Pathophysiology of chaperone-mediated autophagy. *Int J Biochem Cell Biol* **36**(12), 2420-2434
95. Glover J. R., and Lindquist S. (1998) Hsp104, Hsp70, and Hsp40: a novel chaperone system that rescues previously aggregated proteins. *Cell* **94**(1), 73-82
96. Diamant S., Ben-Zvi A. P., Bukau B., and Goloubinoff P. (2000) Size-dependent disaggregation of stable protein aggregates by the DnaK chaperone machinery. *J Biol Chem* **275**(28), 21107-21113
97. Kim S., Nollen E. A., Kitagawa K., Bindokas V. P., and Morimoto R. I. (2002) Polyglutamine protein aggregates are dynamic. *Nat Cell Biol* **4**(10), 826-831
98. Ananthan J., Goldberg A. L., and Voellmy R. (1986) Abnormal proteins serve as eukaryotic stress signals and trigger the activation of heat shock genes. *Science* **232**(4749), 522-524
99. Akerfelt M., Morimoto R. I., and Sistonen L. (2010) Heat shock factors: integrators of cell stress, development and lifespan. *Nat Rev Mol Cell Biol* **11**(8), 545-555
100. Morimoto R. I. (1998) Regulation of the heat shock transcriptional response: cross talk between a family of heat shock factors, molecular chaperones, and negative regulators. *Genes Dev* **12**(24), 3788-3796
101. Magrane J., Smith R. C., Walsh K., and Querfurth H. W. (2004) Heat shock protein 70 participates in the neuroprotective response to intracellularly expressed beta-amyloid in neurons. *J Neurosci* **24**(7), 1700-1706
102. Chai Y., Koppenhafer S. L., Bonini N. M., and Paulson H. L. (1999) Analysis of the role of heat shock protein (Hsp) molecular chaperones in polyglutamine disease. *J Neurosci* **19**(23), 10338-10347
103. Marcuccilli C. J., Mathur S. K., Morimoto R. I., and Miller R. J. (1996) Regulatory differences in the stress response of hippocampal neurons and glial cells after heat shock. *J Neurosci* **16**(2), 478-485

104. Batulan Z., Shinder G. A., Minotti S., He B. P., Doroudchi M. M., Nalbantoglu J., Strong M. J., and Durham H. D. (2003) High threshold for induction of the stress response in motor neurons is associated with failure to activate HSF1. *J Neurosci* **23**(13), 5789-5798

105. Brignull H. R., Moore F. E., Tang S. J., and Morimoto R. I. (2006) Polyglutamine proteins at the pathogenic threshold display neuron-specific aggregation in a pan-neuronal Caenorhabditis elegans model. *J Neurosci* **26**(29), 7597-7606

106. Macario A. J., and Conway de Macario E. (2005) Sick chaperones, cellular stress, and disease. *N Engl J Med* **353**(14), 1489-1501

107. Barral J. M., Broadley S. A., Schaffar G., and Hartl F. U. (2004) Roles of molecular chaperones in protein misfolding diseases. *Semin Cell Dev Biol* **15**(1), 17-29

108. Csermely P. (2001) Chaperone overload is a possible contributor to 'civilization diseases'. *Trends Genet* **17**(12), 701-704

109. Satyal S. H., Schmidt E., Kitagawa K., Sondheimer N., Lindquist S., Kramer J. M., and Morimoto R. I. (2000) Polyglutamine aggregates alter protein folding homeostasis in Caenorhabditis elegans. *Proc Natl Acad Sci U S A* **97**(11), 5750-5755

110. Gidalevitz T., Ben-Zvi A., Ho K. H., Brignull H. R., and Morimoto R. I. (2006) Progressive disruption of cellular protein folding in models of polyglutamine diseases. *Science* **311**(5766), 1471-1474

111. Gidalevitz T., Krupinski T., Garcia S., and Morimoto R. I. (2009) Destabilizing protein polymorphisms in the genetic background direct phenotypic expression of mutant SOD1 toxicity. *PLoS Genet* **5**(3), e1000399

112. Sachidanandam R., Weissman D., Schmidt S. C., Kakol J. M., Stein L. D., Marth G., Sherry S., Mullikin J. C., Mortimore B. J., Willey D. L., Hunt S. E., Cole C. G., Coggill P. C., Rice C. M., Ning Z., Rogers J., Bentley D. R., Kwok P. Y., Mardis E. R., Yeh R. T., Schultz B., Cook L., Davenport R., Dante M., Fulton L., Hillier L., Waterston R. H., McPherson J. D., Gilman B., Schaffner S., Van Etten W. J., Reich D., Higgins J., Daly M. J., Blumenstiel B., Baldwin J., Stange-Thomann N., Zody M. C., Linton L., Lander E. S., and Altshuler D. (2001) A map

of human genome sequence variation containing 1.42 million single nucleotide polymorphisms. *Nature* **409**(6822), 928-933

113. Ng P. C., and Henikoff S. (2006) Predicting the effects of amino acid substitutions on protein function. *Annu Rev Genomics Hum Genet* **7**, 61-80
114. Muchowski P. J., and Wacker J. L. (2005) Modulation of neurodegeneration by molecular chaperones. *Nat Rev Neurosci* **6**(1), 11-22
115. Jana N. R., Tanaka M., Wang G., and Nukina N. (2000) Polyglutamine length-dependent interaction of Hsp40 and Hsp70 family chaperones with truncated N-terminal huntingtin: their role in suppression of aggregation and cellular toxicity. *Hum Mol Genet* **9**(13), 2009-2018
116. Hsu A. L., Murphy C. T., and Kenyon C. (2003) Regulation of aging and age-related disease by DAF-16 and heat-shock factor. *Science* **300**(5622), 1142-1145
117. Kazemi-Esfarjani P., and Benzer S. (2000) Genetic suppression of polyglutamine toxicity in Drosophila. *Science* **287**(5459), 1837-1840
118. Cummings C. J., Sun Y., Opal P., Antalffy B., Mestril R., Orr H. T., Dillmann W. H., and Zoghbi H. Y. (2001) Over-expression of inducible HSP70 chaperone suppresses neuropathology and improves motor function in SCA1 mice. *Hum Mol Genet* **10**(14), 1511-1518
119. McLean P. J., Kawamata H., Shariff S., Hewett J., Sharma N., Ueda K., Breakefield X. O., and Hyman B. T. (2002) TorsinA and heat shock proteins act as molecular chaperones: suppression of alpha-synuclein aggregation. *J Neurochem* **83**(4), 846-854
120. Klucken J., Shin Y., Masliah E., Hyman B. T., and McLean P. J. (2004) Hsp70 Reduces alpha-Synuclein Aggregation and Toxicity. *J Biol Chem* **279**(24), 25497-25502
121. Wyttenbach A., Carmichael J., Swartz J., Furlong R. A., Narain Y., Rankin J., and Rubinsztein D. C. (2000) Effects of heat shock, heat shock protein 40 (HDJ-2), and proteasome inhibition on protein aggregation in cellular models of Huntington's disease. *Proc Natl Acad Sci U S A* **97**(6), 2898-2903

122. Krobitsch S., and Lindquist S. (2000) Aggregation of huntingtin in yeast varies with the length of the polyglutamine expansion and the expression of chaperone proteins. *Proc Natl Acad Sci U S A* **97**(4), 1589-1594

123. Meriin A. B., Zhang X., He X., Newnam G. P., Chernoff Y. O., and Sherman M. Y. (2002) Huntington toxicity in yeast model depends on polyglutamine aggregation mediated by a prion-like protein Rnq1. *J Cell Biol* **157**(6), 997-1004

124. Warrick J. M., Chan H. Y., Gray-Board G. L., Chai Y., Paulson H. L., and Bonini N. M. (1999) Suppression of polyglutamine-mediated neurodegeneration in Drosophila by the molecular chaperone HSP70. *Nat Genet* **23**(4), 425-428

125. Hansson O., Nylandsted J., Castilho R. F., Leist M., Jaattela M., and Brundin P. (2003) Overexpression of heat shock protein 70 in R6/2 Huntington's disease mice has only modest effects on disease progression. *Brain Res* **970**(1-2), 47-57

126. Auluck P. K., Chan H. Y., Trojanowski J. Q., Lee V. M., and Bonini N. M. (2002) Chaperone suppression of alpha-synuclein toxicity in a Drosophila model for Parkinson's disease. *Science* **295**(5556), 865-868

127. Nollen E. A., Garcia S. M., van Haaften G., Kim S., Chavez A., Morimoto R. I., and Plasterk R. H. (2004) Genome-wide RNA interference screen identifies previously undescribed regulators of polyglutamine aggregation. *Proc Natl Acad Sci U S A* **101**(17), 6403-6408

128. Zhang S., Binari R., Zhou R., and Perrimon N. (2010) A genomewide RNA interference screen for modifiers of aggregates formation by mutant Huntingtin in Drosophila. *Genetics* **184**(4), 1165-1179

129. Chan H. Y., Warrick J. M., Gray-Board G. L., Paulson H. L., and Bonini N. M. (2000) Mechanisms of chaperone suppression of polyglutamine disease: selectivity, synergy and modulation of protein solubility in Drosophila. *Hum Mol Genet* **9**(19), 2811-2820

130. Fujimoto M., Takaki E., Hayashi T., Kitaura Y., Tanaka Y., Inouye S., and Nakai A. (2005) Active HSF1 significantly suppresses polyglutamine aggregate formation in cellular and mouse models. *J Biol Chem* **280**(41), 34908-34916

131. Zou J., Guo Y., Guettouche T., Smith D. F., and Voellmy R. (1998) Repression of heat shock transcription factor HSF1 activation by HSP90 (HSP90 complex) that forms a stress-sensitive complex with HSF1. *Cell* **94**(4), 471-480
132. Auluck P. K., and Bonini N. M. (2002) Pharmacological prevention of Parkinson disease in Drosophila. *Nat Med* **8**(11), 1185-1186
133. Fujikake N., Nagai Y., Popiel H. A., Okamoto Y., Yamaguchi M., and Toda T. (2008) Heat shock transcription factor 1-activating compounds suppress polyglutamine-induced neurodegeneration through induction of multiple molecular chaperones. *J Biol Chem* **283**(38), 26188-26197
134. Kieran D., Kalmar B., Dick J. R., Riddoch-Contreras J., Burnstock G., and Greensmith L. (2004) Treatment with arimoclomol, a coinducer of heat shock proteins, delays disease progression in ALS mice. *Nat Med* **10**(4), 402-405
135. Muchowski P. J., Schaffar G., Sittler A., Wanker E. E., Hayer-Hartl M. K., and Hartl F. U. (2000) Hsp70 and hsp40 chaperones can inhibit self-assembly of polyglutamine proteins into amyloid-like fibrils. *Proc Natl Acad Sci U S A* **97**(14), 7841-7846
136. Dedmon M. M., Christodoulou J., Wilson M. R., and Dobson C. M. (2005) Heat shock protein 70 inhibits alpha-synuclein fibril formation via preferential binding to prefibrillar species. *J Biol Chem* **280**(15), 14733-14740
137. Evans C. G., Wisen S., and Gestwicki J. E. (2006) Heat shock proteins 70 and 90 inhibit early stages of amyloid beta-(1-42) aggregation in vitro. *J Biol Chem* **281**(44), 33182-33191
138. Sittler A., Lurz R., Lueder G., Priller J., Lehrach H., Hayer-Hartl M. K., Hartl F. U., and Wanker E. E. (2001) Geldanamycin activates a heat shock response and inhibits huntingtin aggregation in a cell culture model of Huntington's disease. *Hum Mol Genet* **10**(12), 1307-1315
139. Muchowski P. J. (2002) Protein misfolding, amyloid formation, and neurodegeneration: a critical role for molecular chaperones? *Neuron* **35**(1), 9-12
140. Bailey C. K., Andriola I. F., Kampinga H. H., and Merry D. E. (2002) Molecular chaperones enhance the degradation of expanded polyglutamine repeat androgen

receptor in a cellular model of spinal and bulbar muscular atrophy. *Hum Mol Genet* **11**(5), 515-523

141. Kumar P., Ambasta R. K., Veereshwarayya V., Rosen K. M., Kosik K. S., Band H., Mestril R., Patterson C., and Querfurth H. W. (2007) CHIP and HSPs interact with beta-APP in a proteasome-dependent manner and influence Abeta metabolism. *Hum Mol Genet* **16**(7), 848-864
142. Zhou H., Li S. H., and Li X. J. (2001) Chaperone suppression of cellular toxicity of huntingtin is independent of polyglutamine aggregation. *J Biol Chem* **276**(51), 48417-48424
143. Gabai V. L., Meriin A. B., Mosser D. D., Caron A. W., Rits S., Shifrin V. I., and Sherman M. Y. (1997) Hsp70 prevents activation of stress kinases. A novel pathway of cellular thermotolerance. *J Biol Chem* **272**(29), 18033-18037
144. Mosser D. D., Caron A. W., Bourget L., Denis-Larose C., and Massie B. (1997) Role of the human heat shock protein hsp70 in protection against stress-induced apoptosis. *Mol Cell Biol* **17**(9), 5317-5327
145. Park H. S., Lee J. S., Huh S. H., Seo J. S., and Choi E. J. (2001) Hsp72 functions as a natural inhibitory protein of c-Jun N-terminal kinase. *EMBO J* **20**(3), 446-456
146. Liu Y. F. (1998) Expression of polyglutamine-expanded Huntingtin activates the SEK1-JNK pathway and induces apoptosis in a hippocampal neuronal cell line. *J Biol Chem* **273**(44), 28873-28877
147. Merienne K., Helmlinger D., Perkin G. R., Devys D., and Trottier Y. (2003) Polyglutamine expansion induces a protein-damaging stress connecting heat shock protein 70 to the JNK pathway. *J Biol Chem* **278**(19), 16957-16967
148. Lopez Salon M., Pasquini L., Besio Moreno M., Pasquini J. M., and Soto E. (2003) Relationship between beta-amyloid degradation and the 26S proteasome in neural cells. *Exp Neurol* **180**(2), 131-143
149. David D. C., Layfield R., Serpell L., Narain Y., Goedert M., and Spillantini M. G. (2002) Proteasomal degradation of tau protein. *J Neurochem* **83**(1), 176-185
150. Bennett M. C., Bishop J. F., Leng Y., Chock P. B., Chase T. N., and Mouradian M. M. (1999) Degradation of alpha-synuclein by proteasome. *J Biol Chem* **274**(48), 33855-33858

151. Webb J. L., Ravikumar B., Atkins J., Skepper J. N., and Rubinsztein D. C. (2003) Alpha-Synuclein is degraded by both autophagy and the proteasome. *J Biol Chem* **278**(27), 25009-25013

152. Li X., Wang C. E., Huang S., Xu X., Li X. J., Li H., and Li S. (2010) Inhibiting the ubiquitin-proteasome system leads to preferential accumulation of toxic N-terminal mutant huntingtin fragments. *Hum Mol Genet* **19**(12), 2445-2455

153. Ravikumar B., Duden R., and Rubinsztein D. C. (2002) Aggregate-prone proteins with polyglutamine and polyalanine expansions are degraded by autophagy. *Hum Mol Genet* **11**(9), 1107-1117

154. Iwata A., Christianson J. C., Bucci M., Ellerby L. M., Nukina N., Forno L. S., and Kopito R. R. (2005) Increased susceptibility of cytoplasmic over nuclear polyglutamine aggregates to autophagic degradation. *Proc Natl Acad Sci U S A* **102**(37), 13135-13140

155. Cummings C. J., Reinstein E., Sun Y., Antalffy B., Jiang Y., Ciechanover A., Orr H. T., Beaudet A. L., and Zoghbi H. Y. (1999) Mutation of the E6-AP ubiquitin ligase reduces nuclear inclusion frequency while accelerating polyglutamine-induced pathology in SCA1 mice. *Neuron* **24**(4), 879-892

156. Chai Y., Koppenhafer S. L., Shoesmith S. J., Perez M. K., and Paulson H. L. (1999) Evidence for proteasome involvement in polyglutamine disease: localization to nuclear inclusions in SCA3/MJD and suppression of polyglutamine aggregation in vitro. *Hum Mol Genet* **8**(4), 673-682

157. Kabuta T., Suzuki Y., and Wada K. (2006) Degradation of amyotrophic lateral sclerosis-linked mutant Cu,Zn-superoxide dismutase proteins by macroautophagy and the proteasome. *J Biol Chem* **281**(41), 30524-30533

158. Keller J. N., Hanni K. B., and Markesbery W. R. (2000) Impaired proteasome function in Alzheimer's disease. *J Neurochem* **75**(1), 436-439

159. McNaught K. S., and Jenner P. (2001) Proteasomal function is impaired in substantia nigra in Parkinson's disease. *Neurosci Lett* **297**(3), 191-194

160. McNaught K. S., Perl D. P., Brownell A. L., and Olanow C. W. (2004) Systemic exposure to proteasome inhibitors causes a progressive model of Parkinson's disease. *Ann Neurol* **56**(1), 149-162

161. Bedford L., Hay D., Devoy A., Paine S., Powe D. G., Seth R., Gray T., Topham I., Fone K., Rezvani N., Mee M., Soane T., Layfield R., Sheppard P. W., Ebendal T., Usoskin D., Lowe J., and Mayer R. J. (2008) Depletion of 26S proteasomes in mouse brain neurons causes neurodegeneration and Lewy-like inclusions resembling human pale bodies. *J Neurosci* **28**(33), 8189-8198

162. Komatsu M., Waguri S., Chiba T., Murata S., Iwata J., Tanida I., Ueno T., Koike M., Uchiyama Y., Kominami E., and Tanaka K. (2006) Loss of autophagy in the central nervous system causes neurodegeneration in mice. *Nature* **441**(7095), 880-884

163. Hara T., Nakamura K., Matsui M., Yamamoto A., Nakahara Y., Suzuki-Migishima R., Yokoyama M., Mishima K., Saito I., Okano H., and Mizushima N. (2006) Suppression of basal autophagy in neural cells causes neurodegenerative disease in mice. *Nature* **441**(7095), 885-889

164. Ravikumar B., Vacher C., Berger Z., Davies J. E., Luo S., Oroz L. G., Scaravilli F., Easton D. F., Duden R., O'Kane C. J., and Rubinsztein D. C. (2004) Inhibition of mTOR induces autophagy and reduces toxicity of polyglutamine expansions in fly and mouse models of Huntington disease. *Nat Genet* **36**(6), 585-595

165. Berger Z., Ravikumar B., Menzies F. M., Oroz L. G., Underwood B. R., Pangalos M. N., Schmitt I., Wullner U., Evert B. O., O'Kane C. J., and Rubinsztein D. C. (2006) Rapamycin alleviates toxicity of different aggregate-prone proteins. *Hum Mol Genet* **15**(3), 433-442

166. Seo H., Sonntag K. C., Kim W., Cattaneo E., and Isacson O. (2007) Proteasome activator enhances survival of Huntington's disease neuronal model cells. *PLoS One* **2**(2), e238

167. Jana N. R., Dikshit P., Goswami A., Kotliarova S., Murata S., Tanaka K., and Nukina N. (2005) Co-chaperone CHIP associates with expanded polyglutamine protein and promotes their degradation by proteasomes. *J Biol Chem* **280**(12), 11635-11640

168. Al-Ramahi I., Lam Y. C., Chen H. K., de Gouyon B., Zhang M., Perez A. M., Branco J., de Haro M., Patterson C., Zoghbi H. Y., and Botas J. (2006) CHIP

protects from the neurotoxicity of expanded and wild-type ataxin-1 and promotes their ubiquitination and degradation. *J Biol Chem* **281**(36), 26714-26724

169. Adachi H., Waza M., Tokui K., Katsuno M., Minamiyama M., Tanaka F., Doyu M., and Sobue G. (2007) CHIP overexpression reduces mutant androgen receptor protein and ameliorates phenotypes of the spinal and bulbar muscular atrophy transgenic mouse model. *J Neurosci* **27**(19), 5115-5126
170. Huang Q., and Figueiredo-Pereira M. E. (2010) Ubiquitin/proteasome pathway impairment in neurodegeneration: therapeutic implications. *Apoptosis* **15**(11), 1292-1311
171. Nedelsky N. B., Todd P. K., and Taylor J. P. (2008) Autophagy and the ubiquitin-proteasome system: collaborators in neuroprotection. *Biochim Biophys Acta* **1782**(12), 691-699
172. Korolchuk V. I., Menzies F. M., and Rubinsztein D. C. (2010) Mechanisms of cross-talk between the ubiquitin-proteasome and autophagy-lysosome systems. *FEBS Lett* **584**(7), 1393-1398
173. Ding W. X., and Yin X. M. (2008) Sorting, recognition and activation of the misfolded protein degradation pathways through macroautophagy and the proteasome. *Autophagy* **4**(2), 141-150
174. Ciechanover A., and Brundin P. (2003) The ubiquitin proteasome system in neurodegenerative diseases: sometimes the chicken, sometimes the egg. *Neuron* **40**(2), 427-446
175. Verhoef L. G., Lindsten K., Masucci M. G., and Dantuma N. P. (2002) Aggregate formation inhibits proteasomal degradation of polyglutamine proteins. *Hum Mol Genet* **11**(22), 2689-2700
176. Yamamoto A., Lucas J. J., and Hen R. (2000) Reversal of neuropathology and motor dysfunction in a conditional model of Huntington's disease. *Cell* **101**(1), 57-66
177. Martin-Aparicio E., Yamamoto A., Hernandez F., Hen R., Avila J., and Lucas J. J. (2001) Proteasomal-dependent aggregate reversal and absence of cell death in a conditional mouse model of Huntington's disease. *J Neurosci* **21**(22), 8772-8781

178. Iwata A., Riley B. E., Johnston J. A., and Kopito R. R. (2005) HDAC6 and microtubules are required for autophagic degradation of aggregated huntingtin. *J Biol Chem* **280**(48), 40282-40292
179. Pandey U. B., Nie Z., Batlevi Y., McCray B. A., Ritson G. P., Nedelsky N. B., Schwartz S. L., DiProspero N. A., Knight M. A., Schuldiner O., Padmanabhan R., Hild M., Berry D. L., Garza D., Hubbert C. C., Yao T. P., Baehrecke E. H., and Taylor J. P. (2007) HDAC6 rescues neurodegeneration and provides an essential link between autophagy and the UPS. *Nature* **447**(7146), 859-863
180. Fortun J., Dunn W. A., Jr., Joy S., Li J., and Notterpek L. (2003) Emerging role for autophagy in the removal of aggresomes in Schwann cells. *J Neurosci* **23**(33), 10672-10680
181. Kaganovich D., Kopito R., and Frydman J. (2008) Misfolded proteins partition between two distinct quality control compartments. *Nature* **454**(7208), 1088-1095
182. Hipkiss A. R. (2006) Accumulation of altered proteins and ageing: causes and effects. *Exp Gerontol* **41**(5), 464-473
183. Stadtman E. R. (2004) Role of oxidant species in aging. *Curr Med Chem* **11**(9), 1105-1112
184. Friguet B. (2006) Oxidized protein degradation and repair in ageing and oxidative stress. *FEBS Lett* **580**(12), 2910-2916
185. Martinez-Vicente M., Sovak G., and Cuervo A. M. (2005) Protein degradation and aging. *Exp Gerontol* **40**(8-9), 622-633
186. Lindner A. B., and Demarez A. (2009) Protein aggregation as a paradigm of aging. *Biochim Biophys Acta* **1790**(10), 980-996
187. Ben-Zvi A., Miller E. A., and Morimoto R. I. (2009) Collapse of proteostasis represents an early molecular event in Caenorhabditis elegans aging. *Proc Natl Acad Sci U S A* **106**(35), 14914-14919
188. Soti C., and Csermely P. (2000) Molecular chaperones and the aging process. *Biogerontology* **1**(3), 225-233
189. Soti C., and Csermely P. (2003) Aging and molecular chaperones. *Exp Gerontol* **38**(10), 1037-1040

190. Nardai G., Csermely P., and Soti C. (2002) Chaperone function and chaperone overload in the aged. A preliminary analysis. *Exp Gerontol* **37**(10-11), 1257-1262
191. Morley J. F., and Morimoto R. I. (2004) Regulation of longevity in Caenorhabditis elegans by heat shock factor and molecular chaperones. *Mol Biol Cell* **15**(2), 657-664
192. Carrard G., Bulteau A. L., Petropoulos I., and Friguet B. (2002) Impairment of proteasome structure and function in aging. *Int J Biochem Cell Biol* **34**(11), 1461-1474
193. Chondrogianni N., and Gonos E. S. (2005) Proteasome dysfunction in mammalian aging: steps and factors involved. *Exp Gerontol* **40**(12), 931-938
194. Bergamini E., Cavallini G., Donati A., and Gori Z. (2004) The role of macroautophagy in the ageing process, anti-ageing intervention and age-associated diseases. *Int J Biochem Cell Biol* **36**(12), 2392-2404
195. Cuervo A. M., Bergamini E., Brunk U. T., Droge W., Ffrench M., and Terman A. (2005) Autophagy and aging: the importance of maintaining "clean" cells. *Autophagy* **1**(3), 131-140
196. Friguet B., and Szweda L. I. (1997) Inhibition of the multicatalytic proteinase (proteasome) by 4-hydroxy-2-nonenal cross-linked protein. *FEBS Lett* **405**(1), 21-25
197. Tonoki A., Kuranaga E., Tomioka T., Hamazaki J., Murata S., Tanaka K., and Miura M. (2009) Genetic evidence linking age-dependent attenuation of the 26S proteasome with the aging process. *Mol Cell Biol* **29**(4), 1095-1106
198. Vernace V. A., Arnaud L., Schmidt-Glenewinkel T., and Figueiredo-Pereira M. E. (2007) Aging perturbs 26S proteasome assembly in Drosophila melanogaster. *FASEB J* **21**(11), 2672-2682
199. Conconi M., Szweda L. I., Levine R. L., Stadtman E. R., and Friguet B. (1996) Age-related decline of rat liver multicatalytic proteinase activity and protection from oxidative inactivation by heat-shock protein 90. *Arch Biochem Biophys* **331**(2), 232-240

200. Brunk U. T., and Terman A. (2002) The mitochondrial-lysosomal axis theory of aging: accumulation of damaged mitochondria as a result of imperfect autophagocytosis. *Eur J Biochem* **269**(8), 1996-2002
201. Szweda P. A., Camouse M., Lundberg K. C., Oberley T. D., and Szweda L. I. (2003) Aging, lipofuscin formation, and free radical-mediated inhibition of cellular proteolytic systems. *Ageing Res Rev* **2**(4), 383-405
202. Haigis M. C., and Yankner B. A. (2010) The aging stress response. *Mol Cell* **40**(2), 333-344
203. Del Roso A., Vittorini S., Cavallini G., Donati A., Gori Z., Masini M., Pollera M., and Bergamini E. (2003) Ageing-related changes in the in vivo function of rat liver macroautophagy and proteolysis. *Exp Gerontol* **38**(5), 519-527
204. Cuervo A. M., and Dice J. F. (2000) Age-related decline in chaperone-mediated autophagy. *J Biol Chem* **275**(40), 31505-31513
205. Kiffin R., Kaushik S., Zeng M., Bandyopadhyay U., Zhang C., Massey A. C., Martinez-Vicente M., and Cuervo A. M. (2007) Altered dynamics of the lysosomal receptor for chaperone-mediated autophagy with age. *J Cell Sci* **120**(Pt 5), 782-791
206. Morley J. F., Brignull H. R., Weyers J. J., and Morimoto R. I. (2002) The threshold for polyglutamine-expansion protein aggregation and cellular toxicity is dynamic and influenced by aging in Caenorhabditis elegans. *Proc Natl Acad Sci U S A* **99**(16), 10417-10422
207. Zhou H., Cao F., Wang Z., Yu Z. X., Nguyen H. P., Evans J., Li S. H., and Li X. J. (2003) Huntingtin forms toxic NH2-terminal fragment complexes that are promoted by the age-dependent decrease in proteasome activity. *J Cell Biol* **163**(1), 109-118
208. Kawarabayashi T., Younkin L. H., Saido T. C., Shoji M., Ashe K. H., and Younkin S. G. (2001) Age-dependent changes in brain, CSF, and plasma amyloid (beta) protein in the Tg2576 transgenic mouse model of Alzheimer's disease. *J Neurosci* **21**(2), 372-381
209. van Ham T. J., Thijssen K. L., Breitling R., Hofstra R. M., Plasterk R. H., and Nollen E. A. (2008) C. elegans model identifies genetic modifiers of alpha-synuclein inclusion formation during aging. *PLoS Genet* **4**(3), e1000027

210. Wang J., Xu G., and Borchelt D. R. (2002) High molecular weight complexes of mutant superoxide dismutase 1: age-dependent and tissue-specific accumulation. *Neurobiol Dis* **9**(2), 139-148

211. David D. C., Ollikainen N., Trinidad J. C., Cary M. P., Burlingame A. L., and Kenyon C. (2010) Widespread protein aggregation as an inherent part of aging in C. elegans. *PLoS Biol* **8**(8), e1000450

212. Winklhofer K. F., Tatzelt J., and Haass C. (2008) The two faces of protein misfolding: gain- and loss-of-function in neurodegenerative diseases. *EMBO J* **27**(2), 336-349

213. Link C. D., Fonte V., Hiester B., Yerg J., Ferguson J., Csontos S., Silverman M. A., and Stein G. H. (2006) Conversion of green fluorescent protein into a toxic, aggregation-prone protein by C-terminal addition of a short peptide. *J Biol Chem* **281**(3), 1808-1816

214. Robben J., Van der Schueren J., and Volckaert G. (1993) Carboxyl terminus is essential for intracellular folding of chloramphenicol acetyltransferase. *J Biol Chem* **268**(33), 24555-24558

215. Van der Schueren J., Robben J., and Volckaert G. (1998) Misfolding of chloramphenicol acetyltransferase due to carboxy-terminal truncation can be corrected by second-site mutations. *Protein Eng* **11**(12), 1211-1217

216. Tamas P., Solti Z., Bauer P., Illes A., Sipeki S., Bauer A., Farago A., Downward J., and Buday L. (2003) Mechanism of epidermal growth factor regulation of Vav2, a guanine nucleotide exchange factor for Rac. *J Biol Chem* **278**(7), 5163-5171

217. Shaw W. V. (1975) Chloramphenicol acetyltransferase from chloramphenicol-resistant bacteria. *Methods Enzymol* **43**737-755

218. Garcia-Mata R., Bebok Z., Sorscher E. J., and Sztul E. S. (1999) Characterization and dynamics of aggresome formation by a cytosolic GFP-chimera. *J Cell Biol* **146**(6), 1239-1254

219. Westerheide S. D., Bosman J. D., Mbadugha B. N., Kawahara T. L., Matsumoto G., Kim S., Gu W., Devlin J. P., Silverman R. B., and Morimoto R. I. (2004)

Celastrols as inducers of the heat shock response and cytoprotection. *J Biol Chem* **279**(53), 56053-56060

220. Guo Y., Guettouche T., Fenna M., Boellmann F., Pratt W. B., Toft D. O., Smith D. F., and Voellmy R. (2001) Evidence for a mechanism of repression of heat shock factor 1 transcriptional activity by a multichaperone complex. *J Biol Chem* **276**(49), 45791-45799
221. Metzger M. B., and Michaelis S. (2009) Analysis of quality control substrates in distinct cellular compartments reveals a unique role for Rpn4p in tolerating misfolded membrane proteins. *Mol Biol Cell* **20**(3), 1006-1019
222. Geiler-Samerotte K. A., Dion M. F., Budnik B. A., Wang S. M., Hartl D. L., and Drummond D. A. (2011) Misfolded proteins impose a dosage-dependent fitness cost and trigger a cytosolic unfolded protein response in yeast. *Proc Natl Acad Sci U S A* **108**(2), 680-685
223. Michels A. A., Kanon B., Konings A. W., Ohtsuka K., Bensaude O., and Kampinga H. H. (1997) Hsp70 and Hsp40 chaperone activities in the cytoplasm and the nucleus of mammalian cells. *J Biol Chem* **272**(52), 33283-33289
224. Schubert U., Anton L. C., Gibbs J., Norbury C. C., Yewdell J. W., and Bennink J. R. (2000) Rapid degradation of a large fraction of newly synthesized proteins by proteasomes. *Nature* **404**(6779), 770-774
225. Han Y. H., and Park W. H. (2010) MG132 as a proteasome inhibitor induces cell growth inhibition and cell death in A549 lung cancer cells via influencing reactive oxygen species and GSH level. *Hum Exp Toxicol* **29**(7), 607-614
226. Han Y. H., Moon H. J., You B. R., and Park W. H. (2009) The effect of MG132, a proteasome inhibitor on HeLa cells in relation to cell growth, reactive oxygen species and GSH. *Oncol Rep* **22**(1), 215-221
227. Westerheide S. D., Anckar J., Stevens S. M., Jr., Sistonen L., and Morimoto R. I. (2009) Stress-inducible regulation of heat shock factor 1 by the deacetylase SIRT1. *Science* **323**(5917), 1063-1066
228. Donmez G., Arun A., Chung C. Y., McLean P. J., Lindquist S., and Guarente L. (2012) SIRT1 Protects against alpha-Synuclein Aggregation by Activating Molecular Chaperones. *J Neurosci* **32**(1), 124-132

229. Parker J. A., Arango M., Abderrahmane S., Lambert E., Tourette C., Catoire H., and Neri C. (2005) Resveratrol rescues mutant polyglutamine cytotoxicity in nematode and mammalian neurons. *Nat Genet* **37**(4), 349-350

230. Burnett C., Valentini S., Cabreiro F., Goss M., Somogyvari M., Piper M. D., Hoddinott M., Sutphin G. L., Leko V., McElwee J. J., Vazquez-Manrique R. P., Orfila A. M., Ackerman D., Au C., Vinti G., Riesen M., Howard K., Neri C., Bedalov A., Kaeberlein M., Soti C., Partridge L., and Gems D. (2011) Absence of effects of Sir2 overexpression on lifespan in C. elegans and Drosophila. *Nature* **477**(7365), 482-485

231. Kanfi Y., Peshti V., Gil R., Naiman S., Nahum L., Levin E., Kronfeld-Schor N., and Cohen H. Y. (2010) SIRT6 protects against pathological damage caused by diet-induced obesity. *Aging Cell* **9**(2), 162-173

232. Pfister J. A., Ma C., Morrison B. E., and D'Mello S. R. (2008) Opposing effects of sirtuins on neuronal survival: SIRT1-mediated neuroprotection is independent of its deacetylase activity. *PLoS One* **3**(12), e4090

233. Gilon T., Chomsky O., and Kulka R. G. (1998) Degradation signals for ubiquitin system proteolysis in Saccharomyces cerevisiae. *EMBO J* **17**(10), 2759-2766

234. Gilon T., Chomsky O., and Kulka R. G. (2000) Degradation signals recognized by the Ubc6p-Ubc7p ubiquitin-conjugating enzyme pair. *Mol Cell Biol* **20**(19), 7214-7219

235. Bett J. S., Cook C., Petrucelli L., and Bates G. P. (2009) The ubiquitin-proteasome reporter GFPu does not accumulate in neurons of the R6/2 transgenic mouse model of Huntington's disease. *PLoS One* **4**(4), e5128

236. Metzger M. B., Maurer M. J., Dancy B. M., and Michaelis S. (2008) Degradation of a cytosolic protein requires endoplasmic reticulum-associated degradation machinery. *J Biol Chem* **283**(47), 32302-32316

237. Trotter E. W., Kao C. M., Berenfeld L., Botstein D., Petsko G. A., and Gray J. V. (2002) Misfolded proteins are competent to mediate a subset of the responses to heat shock in Saccharomyces cerevisiae. *J Biol Chem* **277**(47), 44817-44825

238. Sugio A., Dreos R., Aparicio F., and Maule A. J. (2009) The cytosolic protein response as a subcomponent of the wider heat shock response in Arabidopsis. *Plant Cell* **21**(2), 642-654

239. Takamiya R., Takahashi M., Park Y. S., Tawara Y., Fujiwara N., Miyamoto Y., Gu J., Suzuki K., and Taniguchi N. (2005) Overexpression of mutated Cu,Zn-SOD in neuroblastoma cells results in cytoskeletal change. *Am J Physiol Cell Physiol* **288**(2), C253-259

240. Trotter E. W., Berenfeld L., Krause S. A., Petsko G. A., and Gray J. V. (2001) Protein misfolding and temperature up-shift cause G1 arrest via a common mechanism dependent on heat shock factor in Saccharomycescerevisiae. *Proc Natl Acad Sci U S A* **98**(13), 7313-7318

241. Olzscha H., Schermann S. M., Woerner A. C., Pinkert S., Hecht M. H., Tartaglia G. G., Vendruscolo M., Hayer-Hartl M., Hartl F. U., and Vabulas R. M. (2011) Amyloid-like aggregates sequester numerous metastable proteins with essential cellular functions. *Cell* **144**(1), 67-78

242. Feder J. H., Rossi J. M., Solomon J., Solomon N., and Lindquist S. (1992) The consequences of expressing hsp70 in Drosophila cells at normal temperatures. *Genes Dev* **6**(8), 1402-1413

243. Song J., Takeda M., and Morimoto R. I. (2001) Bag1-Hsp70 mediates a physiological stress signalling pathway that regulates Raf-1/ERK and cell growth. *Nat Cell Biol* **3**(3), 276-282

244. Loo D. T., Copani A., Pike C. J., Whittemore E. R., Walencewicz A. J., and Cotman C. W. (1993) Apoptosis is induced by beta-amyloid in cultured central nervous system neurons. *Proc Natl Acad Sci U S A* **90**(17), 7951-7955

245. El-Agnaf O. M., Jakes R., Curran M. D., Middleton D., Ingenito R., Bianchi E., Pessi A., Neill D., and Wallace A. (1998) Aggregates from mutant and wild-type alpha-synuclein proteins and NAC peptide induce apoptotic cell death in human neuroblastoma cells by formation of beta-sheet and amyloid-like filaments. *FEBS Lett* **440**(1-2), 71-75

246. Rabizadeh S., Gralla E. B., Borchelt D. R., Gwinn R., Valentine J. S., Sisodia S., Wong P., Lee M., Hahn H., and Bredesen D. E. (1995) Mutations associated with

amyotrophic lateral sclerosis convert superoxide dismutase from an antiapoptotic gene to a proapoptotic gene: studies in yeast and neural cells. *Proc Natl Acad Sci U S A* **92**(7), 3024-3028

247. Kern A., Ackermann B., Clement A. M., Duerk H., and Behl C. (2010) HSF1-controlled and age-associated chaperone capacity in neurons and muscle cells of C. elegans. *PLoS One* **5**(1), e8568

248. Jiang M., Wang J., Fu J., Du L., Jeong H., West T., Xiang L., Peng Q., Hou Z., Cai H., Seredenina T., Arbez N., Zhu S., Sommers K., Qian J., Zhang J., Mori S., Yang X. W., Tamashiro K. L., Aja S., Moran T. H., Luthi-Carter R., Martin B., Maudsley S., Mattson M. P., Cichewicz R. H., Ross C. A., Holtzman D. M., Krainc D., and Duan W. (2012) Neuroprotective role of Sirt1 in mammalian models of Huntington's disease through activation of multiple Sirt1 targets. *Nat Med* **18**(1), 153-158

249. Albani D., Polito L., Batelli S., De Mauro S., Fracasso C., Martelli G., Colombo L., Manzoni C., Salmona M., Caccia S., Negro A., and Forloni G. (2009) The SIRT1 activator resveratrol protects SK-N-BE cells from oxidative stress and against toxicity caused by alpha-synuclein or amyloid-beta (1-42) peptide. *J Neurochem* **110**(5), 1445-1456

250. Kim D., Nguyen M. D., Dobbin M. M., Fischer A., Sananbenesi F., Rodgers J. T., Delalle I., Baur J. A., Sui G., Armour S. M., Puigserver P., Sinclair D. A., and Tsai L. H. (2007) SIRT1 deacetylase protects against neurodegeneration in models for Alzheimer's disease and amyotrophic lateral sclerosis. *EMBO J* **26**(13), 3169-3179

251. Brooks C. L., and Gu W. (2009) How does SIRT1 affect metabolism, senescence and cancer? *Nat Rev Cancer* **9**(2), 123-128

252. Haigis M. C., and Sinclair D. A. (2010) Mammalian sirtuins: biological insights and disease relevance. *Annu Rev Pathol* **5**, 253-295

253. Ghosh H. S., Spencer J. V., Ng B., McBurney M. W., and Robbins P. D. (2007) Sirt1 interacts with transducin-like enhancer of split-1 to inhibit nuclear factor kappaB-mediated transcription. *Biochem J* **408**(1), 105-111

254. Vaitiekunaite R., Butkiewicz D., Krzesniak M., Przybylek M., Gryc A., Snietura M., Benedyk M., Harris C. C., and Rusin M. (2007) Expression and localization of

Werner syndrome protein is modulated by SIRT1 and PML. *Mech Ageing Dev* **128**(11-12), 650-661

255. Campagna M., Herranz D., Garcia M. A., Marcos-Villar L., Gonzalez-Santamaria J., Gallego P., Gutierrez S., Collado M., Serrano M., Esteban M., and Rivas C. (2011) SIRT1 stabilizes PML promoting its sumoylation. *Cell Death Differ* **18**(1), 72-79
256. Lavu S., Boss O., Elliott P. J., and Lambert P. D. (2008) Sirtuins--novel therapeutic targets to treat age-associated diseases. *Nat Rev Drug Discov* **7**(10), 841-853
257. Drummond D. A., and Wilke C. O. (2008) Mistranslation-induced protein misfolding as a dominant constraint on coding-sequence evolution. *Cell* **134**(2), 341-352
258. Dai C., Whitesell L., Rogers A. B., and Lindquist S. (2007) Heat shock factor 1 is a powerful multifaceted modifier of carcinogenesis. *Cell* **130**(6), 1005-1018

10. Publication List

10.1. Publications related to the thesis

Arslan M. A., Chikina M., Csermely P., Sőti C. (2012) Misfolded proteins inhibit proliferation and promote stress-induced death in SV40-transformed mammalian cells. *FASEB J* **26**(2), 766-777

IF: 6.515

Arslan M. A., Csermely P., Sőti C. (2006) Protein homeostasis and molecular chaperones in aging. *Biogerontology* **7**(5-6), 383-389

IF: 2.125

10.2. Publications not directly related to the thesis

Spiró Z., **Arslan M. A.**, Somogyvári M., Nguyen M. T., Smolders A., Dancsó B., Németh N., Elek Z., Braeckman B., Csermely P., Sőti C. (2012) RNA interference links oxidative stress to the inhibition of heat stress adaptation. *Antioxid Redox Signal* (accepted manuscript DOI: 10.1089/ars.2011.4161) 2012 Feb 27 [Epub ahead of print]

IF: 8.209

Dancsó B., Spiró Z., **Arslan M. A.**, Nguyen M. T., Papp D., Csermely P., Sőti C. (2010) The heat shock connection of metabolic stress and dietary restriction. *Curr Pharm Biotechnol* **11**(2), 139-145

IF: 3.455

Arslan M. A., Kütük Ö., Başağa H. (2006) Protein kinases as drug targets in cancer. *Curr Cancer Drug Targets* **6**(7), 623-634

IF: 5.677

11. Acknowledgements

First of all, I would like to thank my supervisor Dr. Csaba Sőti for his effective guidance throughout the course of this study and for his firm belief in me even at the hardest times. I would like to express my sincere gratitude to Prof. József Mandl for providing me with the opportunity to work at the Department of Medical Chemistry. I am also deeply grateful to Prof. Péter Csermely for critically reading my manuscript and contributing with his invaluable ideas. For the generous support of my studies, I would like to acknowledge the EU PROTEOMAGE Project FP6-518230.

Herein, I would like to thank the present and past members of our laboratory: Beatrix Gilányi for her precious technical support; Minh Tú Nguyen, Diána Papp, Milán Somogyvári, Balázs Dancsó, Zoltán Spiró and Ákos Putics for experimental help as well as for their useful comments and suggestions. I am also grateful to all my colleagues working at the Department of Medical Chemistry for their help and understanding.

Finally, I would like to express my special and deepest thanks to my family for their love, encouragement and support.